Papers in Palaeontology, 2022, https://doi.org/10.1002/spp2.1464

Not a jaguar after all? Phylogenetic affinities and morphology of the Pleistocene felid *Panthera gombaszoegensis*

Narimane Chatar[1,*], Margot Michaud[2], Valentin Fischer[1]

[1] Evolution and Diversity Dynamics Lab, Université de Liège, Belgium, ORCiD: 0000-0003-0449-8574 (NC) and 0000-0002-8808-6747 (VF)

[2] Department of African Zoology, Royal Museum for Central Africa, Tervuren, Belgium, ORCiD: 0000-0001-7075-9862

* Corresponding author: narimane.chatar@uliege.be

Abstract

Panthera gombaszoegensis is a fossil pantherine from the Pleistocene of Eurasia. It has been considered to be the closest ancestor the jaguar (*Panthera onca)* due to dental similarities, and has even sometimes been considered to be a subspecies of jaguar. However, our knowledge of this taxon is limited by the scarcity of cranial remains, which has made it difficult to properly assess the phylogenetic affinities and possible ecological role of this taxon. Here, we describe a new cranium of *P. gombaszoegensis* from Belgium, and present a morphometric analysis of the cranium and dentition of extinct and extant pantherines. Whereas the lower dentition of *P. gombaszoegensis* is similar to that of *P. onca*, similarities were not recovered in other parts of the skull. Some cranial traits of *P. gombaszoegensis* resemble those of other pantherines, especially larger species such as the tiger (*P. tigris*). Some similarities with taxa such as tigers (*P. tigris*), lions (*P. leo*), and leopards (*P. pardus*) in the skull of *P. gombaszoegensis,* suggesting a diet adapted to a wide prey spectrum. The first ever assessment of the phylogenetic placement of *P. gombaszoegensis* places this taxon closer to *P. tigris* than to *P. onca*, which considerably simplifies the biogeographic history of pantherines.

Key words: *Panthera*; morphometry; phylogeny; *gombaszoegensis*; jaguar.

Introduction

Pantherinae, also known as the 'big cats', is a group of apex predators that dominate food chains in every region they are found. The subfamily includes the living lion (*Panthera leo*), tiger (*Panthera tigris*), jaguar (*Panthera onca*), leopard (*Panthera pardus*) and snow leopard (*Panthera uncia*) (Turner & Antón 1997). Pantherines colonised a wide range of habitats since their first appearance, from the tropical rainforests of South America (jaguar, *Panthera onca* Seymour 1989) to the Himalayan peaks (snow leopard, *Panthera uncia* Janečka *et al.* 2008). The putatively oldest pantherine, '*Panthera' blythae*, was found in the Zanda Basin of the north western Himalaya Range, and is approximately 6 million years (Myr) old (Tseng *et al.* 2013). However, it is not considered as a true pantherine by all authors (see Geraads & Peigné 2017), although pantherines likely originated in the central–northern Asia elsewhere in the Holarctic (Mazák 2010; Tseng *et al.* 2013). Pantherines became widespread during a series of Pliocene–Pleistocene migration events (Johnson *et al.* 2006), the first pantherinae arriving in Europe being the large-bodied cat known as *Panthera gombaszoegensis* during the Early Pleistocene (O'Regan & Turner 2004). *Panthera gombaszoegensis* had a wide geographical range (Fig. 1A), potentially due to the absence of competitors until the faunal turnover that took place during the Early/Middle Pleistocene transition when *Panthera leo* and *Panthera pardus* migrated into Europe (O'Regan & Turner 2004; Hemmer & Kahlke 2005). Often called the 'European jaguar' or the 'Eurasian jaguar', *P. gombaszoegensis* was a medium-to-large pantherine which went extinct approximately 350 thousand years (kyr) ago and is commonly considered as the ancestor of the extant jaguar, *Panthera onca* (Hemmer 1981; Hemmer *et al.* 2001; O'Regan & Turner 2004).

Initially regarded as a singular pantherine species (Kretzoi 1938*a*), *P. gombaszoegensis* was later reclassified as a subspecies of the modern jaguar: *Panthera onca gombaszoegensis* (Hemmer 1971). The status of the taxon is still debated, with a series of studies regarding *P. gombaszoegensis* as a fully valid species (Argant & Argant 2011; Reynolds 2013; Marciszak 2014; Stimpson *et al.* 2015; Jiangzuo & Liu 2020), whereas others note that the differences between *P. gombaszoegensis* and the living jaguar are not sufficient to warrant full specific distinction (Hemmer *et al.* 2001, 2010; Hankó 2007; Mol *et al.* 2011). The scarcity of *P. gombaszoegensis* material has made it difficult to unravel this taxonomic debate, especially as the species was erected solely based on isolated teeth described by Kretzoi (1938b) and almost all the material ever reported in the literature is composed of dental remains. It was recently demonstrated that dental traits of *P. onca* and *P. gombaszoegensis* are morphologically different (Jiangzuo & Liu 2020), although the cranial anatomy of *P. gombaszoegensis* remains insufficiently

described in the literature to draw definitive conclusions. As a result, there are very few truly multivariate morphometric analyses comparing *P. gombaszoegensis* to other pantherine species (Mazák, Christiansen, & Kitchener 2011), with most studies limited to bivariate analyses (Langlois 2002; O'Regan & Turner 2004; Argant & Argant 2011; Mol *et al.* 2011; Jiangzuo & Liu 2020; Marciszak & Lipecki 2021). Moreover, the very fragmentary state of fossils assigned to *P. gombaszoegensis* resulted in an absence of this taxon in phylogenetic analyses of pantherines. Indeed Christiansen (2008), Tseng *et al.* (2013), and King & Wallace (2014) have systematically excluded *P. gombaszoegensis* from cladistic datasets due to the amount of missing data.

In this study, we present well-preserved, as-yet undescribed material of *P. gombaszoegensis,* unearthed during the 1980's from 'La Belle-Roche' in southern Belgium (Fig. 1B). We posit that this material can shed light on this obscure taxon, and may help resolve the phylogenetic relationships of this taxon within the Pantherinae. We hereby provide the first comparative description of the craniomandibular anatomy of *P. gombaszoegensis*, and assess its relationship with the modern jaguar *P. onca* and with other extant pantherines, both in terms of phylogeny, morphometry, and ecology.

Material and methods

Institutional abbreviations

AMNH American Museum of Natural History (New York, USA); **IMNH** Idaho Museum of Natural History; **IVPP** Institute of Vertebrate Palaeontology and Palaeoanthropology; **MAV** Museo Anatómico de la Universidad de Valladolid; **MNCN** Museo Nacional de Ciencias Naturales (Madrid, Spain); **MNHN** Museum National d'Histoire Naturelle (Paris, France); **PMU** Paleontological Museum Uppsala universitet (Uppsala, Sweden); **RMCA** Royal Museum for Central Africa; **ULgPA** Université de Liège, palaeontology collections.

Fossil locality

'La Belle-Roche' is a fossil site located in the Belgian province of Liège (Municipality of Sprimont, Belgium), 20 km south of Liège, and a couple of kilometres away from the town of Sprimont (Fig. 1B). In 'La Belle-Roche' (translated as 'The Beautiful Rock'), mudstone deposits filled a karstic cavity carved into Carboniferous limestone (Cordy *et al.* 1993). Uranium–thorium dating provides a minimum age of 350 kyr for the mudstone deposit and fossils it contains (Gascoyne & Schwarcz 1985). The presence of *Ursus deningeri* and *P. gombaszoegensis* indicates the mudstone may have been deposited in an earlier part of the Middle Pleistocene (Roebroeks & Stapert 1986), with estimations reaching 500 kyr (Cordy & Ulrix-Closset 1991; Draily & Cordy 1997).

***Figure 1**: **A**, Occurrences of* P. gombaszoegensis *compared to the historic extent of the extant* P. onca *and* P. tigris*, estimated since 1900 based on Luo et al. (2004) and Seymour (1989). **B**, Location of the 'La Belle-Roche' fossil site, Belgium. Animal silhouettes were obtained from PhyloPic (phylopic.org). Image credits: Manabu Sakamoto (*P. onca*) and Sarah Werning (*P. tigris*).*

Even though ‘La Belle-Roche’ is the only known Belgian fossil site were *P. gombaszoegensis* has been recorded, its presence can be inferred in Belgium before the deposits of ‘La Belle-Roche’, as suggested by the estimated distribution in Europe from 2 Myr in the surrounding countries (Fig. 1A and Fig. S1). Although most of the material from ‘La Belle-Roche’ is extremely fragmentary, this site has yielded a nearly complete cranium of *P. gombaszoegensis* (ULg PA BRII-81-146) and three fragmentary dentaries (ULg-PA-BR-III-M13-79; ULg-PA-20210823-01; ULg-PA-BRII-455). Well-preserved cranial material of *P. gombaszoegensis* is rare (see Plate 1 from Argant & Argant 2011 and Figure 3 A1–3 from Jiangzuo & Liu 2020), and the cranium from ‘La Belle-Roche’ is probably the most complete known to this date.

Material

The cranium of *P. gombaszoegensis* ULg-PA-BR-II-81-146 described in this contribution (Fig. 2A–B and Fig. S2) belongs to the collections of the University of Liège, and is currently exhibited in Le Grand Curtius Museum (Liège, Belgium). Three mandibular fragments were also found at La Belle-Roche: two fragmentary right dentaries ULg-PA-BR-III-M13-79 and ULg-PA-20210823-01, and a fragmentary left dentary ULg-PA-BRII-455 (Fig. 2C–E and Fig. S3). The dentary fragments also belong to the collections of the University of Liège; however, ULg-PA-BRII-455 is currently on display at the Musée du Pays d'Ourthe-Amblève, with ULg-PA-BR-III-M13-79 housed in Le Grand Curtius Museum. For comparative analyses, different extant pantherines from the Museum National d’Histoire Naturelle (MNHN, Paris, France) and the Royal Museum for Central Africa (AfricaMuseum, Tervuren, Belgium) as well as *P. palaeosinensis* from the Paleontological Museum Uppsala universitet (PMU, Uppsala, Sweden), were studied (Table S2 ESM). A three-dimensional (3D) scanned model of a leopard *P. pardus* from the American Museum of Natural History (New York, United States) was downloaded from MorphoSource (media M7779; see Tseng *et al*. (2016) for the original publication of the 3D model), as well as a 3D model of the cranium of the cave lion *P. spelaea* from the Idaho Museum of Natural History, initially published in Melchionna *et al.* (2021). All specimens were adult based on their deciduous dentition; wild caught specimens were preferred for extant species, and we excluded animals with visible dental wear from the study.

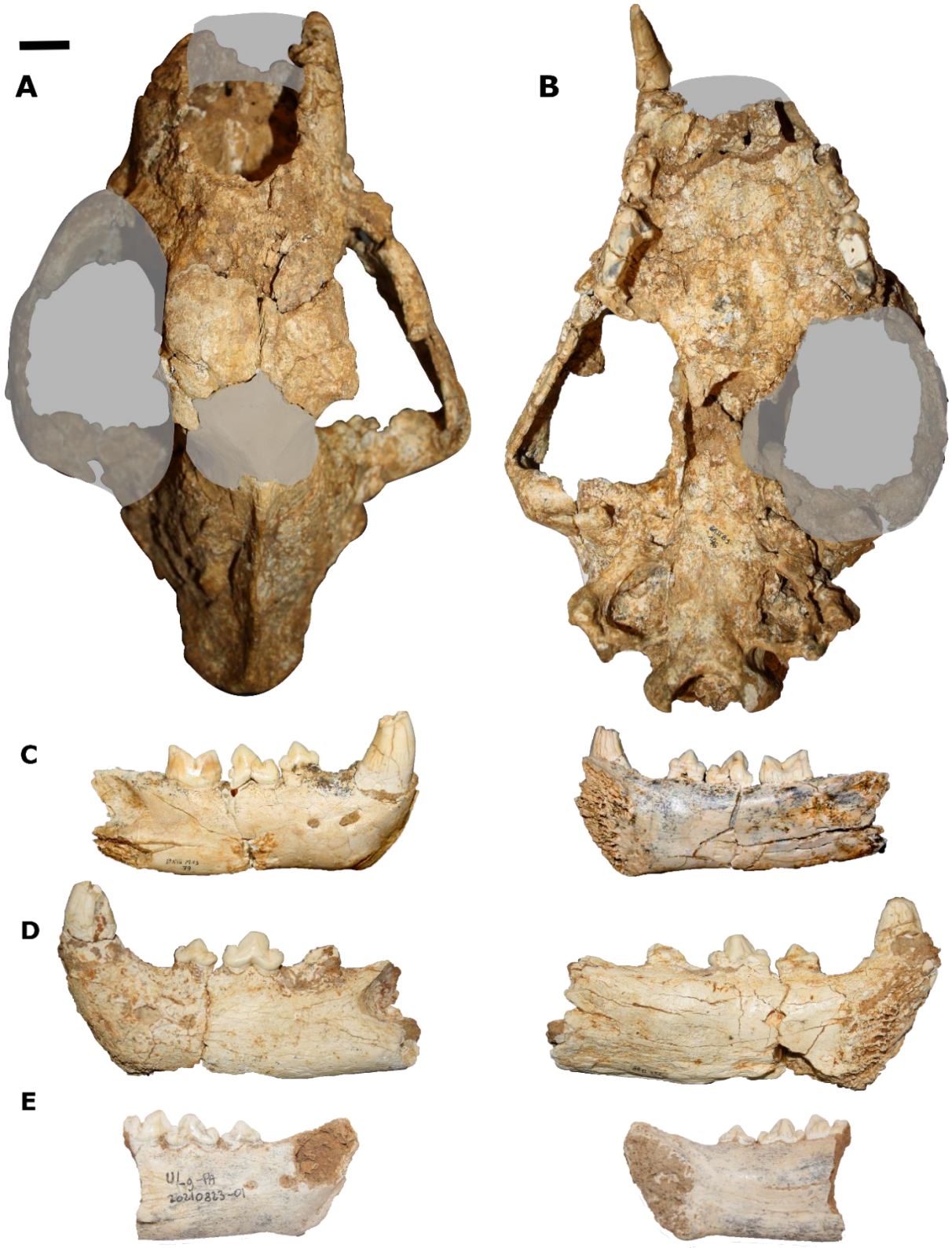

***Figure 2**: Fossil material of* P. gombaszogensis *from la Belle-Roche. Cranium ULg PA BR-II-81-146 in **A**, dorsal and **B**, ventral view. **C-E** mandibular fragments. **C** ULg-PA-BR-III-M13-79, **D** ULg-PA-BRII-455, **E** ULg-PA-20210823-01. Scale bars represent 2cm*

3D data acquisition

In order to compare the different pantherine specimens, material from fossil and extant species were scanned using a Creaform HandySCAN 300 laser surface scanner with a 0.2 mm resolution. 3D models associated with this study are available on Morphosource (Project ID: 000445179, https://www.morphosource.org/projects/000445179?locale=en); models include four specimens of *P. gombaszoegensis* (ULg-PA-BR-II-81-146; ULg-PA-BRII-455; ULg-PA-BR-III-M13-79; ULg-PA-20210823-01), two specimens of *P. spelaea* from the University of Liège (ULg-PA-SCHM-II-14-11; ULg-PA-BRIII-L14-5), and one specimen of *P. palaeosinensis* from the Paleontological Museum Uppsala (cranium PMU 21780/1 and mandible PMU 21780/2).

Phylogenetic analyses

Our phylogenetic analyses are based on the morphological character matrix published by Tseng *et al.* (2013) including fossil and extant pantherines with *Neofelis nebulosa* (the clouded leopard), *Leopardus pardalis* (the ocelot) and *Puma concolor* (The mountain lion) as outgroups. We added *P. gombaszoegensis* as a new OTU and added a new morphological character (Character 40: Contact between both occipital condyles on the ventral part of the cranium: 0 absent, 1 present). We also revised the score of *P. uncia* for the character 1 (position of the nasal-frontal suture), as we observed contradicting character states in one of our specimens. Character 1 for *P. uncia* is now scored as a polymorphism (state 0&1). Our first-hand observations of *P. palaeosinensis* (specimen PMU 21780/1-2) allowed us to score two additional characters states in the matrix of Tseng *et al.* (2013): character 27 (Jugal-Maxillary suture, medial side) as “suture extends posteriorly, then cuts ventrally at the base of the zygomatic arch” (state 0), and the character 58 (Upper canine labial ridges) as “present” (state 1). In addition, we discretised character 48 (P3 parastyle size compared to P3 length), placing the limit between ‘short’ and ‘long’ at 0.5 relative to P3 length as often seen in the literature. Finally, we modified character 42 (Mandibular symphysis angle relative to horizontal ramus) as the previous character states (0: Anteriorly inclined (> 130°) and 1: Weakly inclined (110-120°)) could not be scored for *P. gombaszoegensis* since all the angles we measured were comprised between 120 and 130° (120.400, 127.558, 128.867 124.764, 122.677, 127.335, 128.994, mean = 125.799°). We therefore slightly modified the states to 0: Anteriorly inclined (> 121°) and 1: Weakly inclined (110-120°). The matrix was generated using Mesquite V3 (Maddison & Maddison 2019).

We used TNT v 1.5 (Goloboff & Catalano 2016) to perform the phylogenetic analysis under implied weighting (see appendix S1 for the script). We employed a molecular scaffold to constrain the tree topology, according to the recent

molecular analyses which included fossil taxa (Barnett *et al.* 2016). We expanded the memory of TNT to a maximum of 100,000 trees. We set the search parameters at: New Technology Search, 200 ratchet iterations, 10 cycles of drifting, 5 hits and 5 replications for each hit. We then used the tree branch bisection and reconnection algorithm (TBR) to fully explore the tree islands identified by the ratchet. Nodal support was measured using symmetric resampling with 1000 replications, each replication involving a New Technology search with a change probability of 33%. We choose symmetric resampling over bootstrapping or jack-knifing, as this measure is not affected by character weighting and is thus more appropriate to deal with implied weights (Goloboff *et al.* 2003) (See ESM for the TNT scripts). To test for the influence of character weighting, we ran these analyses with increasing value of the concavity constant K (K=3, 6, 9, and 12). Increasing the value of K reduces the penalty applied to homoplastic characters; however, all the described analyses retrieved the same tree topology.

The best score was obtained when K was set to 12 so we computed the time calibration on the strict consensus cladogram for K=12. To do so, we used the 'equal' method of the 'timePaleoPhy' function from the strap v1.4 package in R (Bell & Lloyd 2015) and a dataset describing the temporal biozones of each OTU (See table S9 for the FAD, LAD and each reference used to estimate the temporal distribution). We then generated the time tree using the 'geoscalePhylo' function from the paleotree v3.3.25 package (Bapst 2012). Ancestral states were reconstructed using Mesquite.

Morphological data

Anatomical descriptions are based on previous research (Barone 1986; Schaller *et al.* 2007; Evans & Lahunta 2013; Jennings & Reighard 2019) and we used the terminology recommended by the *Nomina Anatomica Veterinaria* (2012). Figure S4 shows the main terms used in the description, based on an extant specimen of *P. tigris* (collection ID: MNHN-ZM-AC1931-60).

Multiple measurements were taken capturing the overall shape of the upper dentition (10 measurements, Fig. 3A), lower dentition (9 measurements, Fig. 3B), and cranium (13 measurements, Fig. 3C–E) of the material from La Belle-Roche and other extant and fossil pantherines. To complete our dataset, measurements published by O'Regan (2002) and Jiangzuo & Liu (2020) on the upper dentition were also included in the morphometric analysis (see Table S2). All measurements and ratios on the cranium and on the upper and lower dentition are provided in the supplementary material (Tables S3–S8). All measurements were taken on 3D meshes derived from scanning using the software GOM Inspect suite 2020 (Gesellschaft für Optische Messtechnik, Germany 2020).

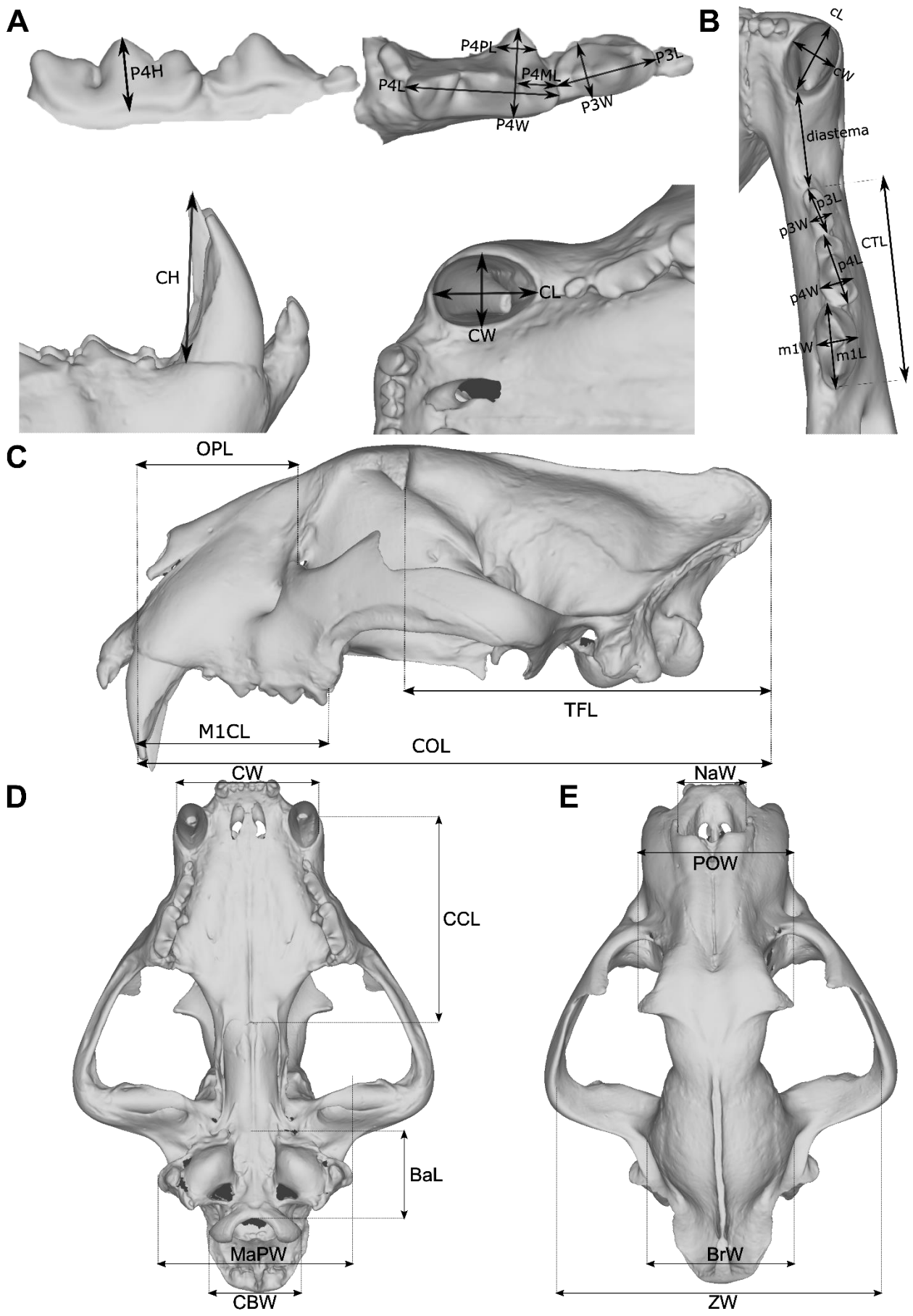
A
P4H
P4PL
P4ML
P3L
P4L
P3W
P4W
CH
CL
CW
B
CL
CW
diastema
p3L
p3W
CTL
p4L
p4W
m1W
m1L
C
OPL
TFL
M1CL
COL
D
CW
CCL
BaL
MaPW
CBW
E
NaW
POW
BrW
ZW

***Figure 3**: 3D model of the cranium and mandible of Panthera tigris MNHN-ZM-AC-1931-60 showing the different measurements taken on **A**, the upper dentition; **B**, the lower dentition and **C-E**, views of the cranium: **C**, lateral; **D**, ventral; **E**, dorsal. Abbreviations : **BaL**, Basioccipital + Basisphenoid length; **BrW**, Maximum braincase width; **CBW**, Condylobasal maximum width; **CCL**, Canine to choanae length; **CH**, Upper canine height; **cL**, lower canine anteroposterior length; **CL**, Upper canine anteroposterior length; **COL**, Canine to occiput length; **CTL**, Cheek teeth anteroposterior length; **cW**, lower canine width; **CW**, Upper canine width; **diastema**, diastema length; **MaPW**, Mastoid process maximum width; **M1CL**, length from M1 to C; **m1L**, lower first molar length; **m1W**, lower first molar width; **NaW**, Nasal width; **OPL**, Orbit to premaxilla length; **POW**, Post-orbital process width; **p3L**, lower third premolar length; **P3L**, Upper third premolar length; **p3W**, lower third premolar width; **P3W**, Upper third width; **P4H**, Upper fourth premolar height; **p4L**, lower fourth premolar length; **P4L**, Upper fourth premolar length; **P4ML**, Upper fourth premolar metacone length; **P4PL**, Upper fourth premolar paracone length; **p4W**, lower fourth premolar width; **P4W**, Upper fourth premolar width; **TFL**, Temporal fossa length; **ZW**, zygomatic width.*

Morphometric analyses

All morphometric analyses were run using the R statistical environment (version 4.0.5; 2021-03-31) (R Core Team 2021). The R script used to run the analysis is provided in the electronic supplementary material. The morphological dataset was imported using the 'read.csv' function and following the protocol published in Fischer *et al.* (2017). We applied a 50% completeness threshold on every specimen to avoid distortion of morphospace due to missing data from incomplete specimens. After applying this threshold, the upper dentition dataset contained 72 specimens out of the 96 measured. All the specimens from the lower dentition (20 specimens) and the cranial measurements dataset (17 specimens) passed the completeness threshold.

The morphological variables of each dataset were then scaled (z-transform), and distance matrices (based on pairwise dissimilarities) were computed from these scaled datasets using the 'dist' function from the stats v4.3.0 package, which uses Euclidean distances as suggested by Legendre & Legendre (1998, pp 424-444). We generated morphospaces using two distinct ordination methods, both capable of handling missing values: a Principal Coordinates Analysis (PCoA), using the 'pcoa' function implemented in the ape v5.5 package (Paradis & Schliep 2019), and a non-metric multidimensional scaling (NMDS), using the 'metaMDS' function of the vegan v2.5-7 package (Dixon 2003). To estimate the influence of the allometric component in our dataset we used a loop to perform a linear regression between the first 10 PCo axes of each dataset and a variable representative of the size (Canine to occiput length, lower canine length and upper canine length). For the upper and lower dentition datasets, a permutational multivariate analysis of variance (PerMANOVA, formerly known as non-parametric / NP-MANOVA) (Anderson 2001) was performed using the 'adonis2' function from the vegan v2.5-7 package

(Dixon 2003). PerMANOVA was performed (1000 permutations using the 'euclidean' method) on the distance matrix of the ratios to test for significant differences between *P. gombaszoegensis* and the other pantherines and we performed post hoc corrections on the significant p-values using the False discovery rate (fdr) correction through the method argument from the 'p.adjust' function in the stats v3.6.2 package.

Systematic palaeontology

MAMMALIA Linnaeus, 1758

CARNIVORA Bowdich, 1821

FELIFORMIA Kretzoi, 1945

FELIDAE Fischer, 1821

FELINAE Fischer, 1821

Genus *PANTHERA* Oken, 1816

Panthera gombaszoegensis Kretzoi, 1938b

Holotype. B991, a series of isolated teeth: C, c, P4, p3 and two m1 illustrated in Kretzoi (1938b).

Emended diagnosis. The P4 ectoparastyle is present with a straight anterior edge and a curved metacone. The P3 has variable anterior and posterior cusps, but usually large with a pronounced cingulum. Vertical groove on the upper canine may be present or indiscernible. Large sagittal crest and strong nuchal crest; vertically oriented occipital condyles; upper incisors positioned in a straight line, with I3 being the largest; large oval-shaped mystacial foramen; wide nasal aperture; nasal bones extend to or beyond the frontomaxillary suture. The m1 protoconid larger than the paraconid; cingulum usually present; talonid very rare. The p4 has a large protocone; anterior and posterior cusps and cingulum are distinct and usually large. The p3 is highly variable, although cusps usually ill-defined with a small posterior cusp. There are no determining features on the mandible, but all specimens have two mental foramina and usually have a straight (but not vertical) symphysis.

Note. A well-defined vertical groove on the upper canine was previously listed in the diagnosis of *P. gombaszoegensis*, but our observation suggests this feature is variable. For this reason, we have emended the diagnosis of *P. gombaszoegensis*.

Type locality and horizon. Gombasek, Slovakia. Gombasek Quarry, Cave deposit, Middle Pleistocene.

Newly referred material. ULg PA BR-II-81-146, ULg-PA-BRII-455, ULg-PA-BR-III-M13-79, ULg-PA-20210823-01.

Comparative description

As Jiangzuo and Liu (2020) recently provided a comprehensive description of the dentition of *P. gombaszoegensis*, we focused on the cranium for the description in this contribution. The mandibular fragments from 'La Belle Roche' are not well preserved enough to

be described here, but there is a recent description of mandibular remains of this taxon published by Jiangzuo *et al.* (2022). A more detailed and complete comparative work should be done on the mandibular anatomy could be done including the new material described by Jiangzuo *et al.* (2022) by also other well preserved material such as the complete left dentary figured in Langlois (2002).

General state of preservation

The cranium ULg PA BR-II-81-146 is relatively complete and is mostly three dimensionally preserved (Fig. 2A–B and S2). It lacks parts of both nasals, pieces of both premaxillae, both pterygoid flanges, and both auditory bullae. The skull is slightly distorted mainly due to a minimal rotation of the palatal region. Moreover, it is worth noting that the anterior-most section of both parietals is restored in plaster (Fig. 2). Due to some parts of bones being missing, some measurements for the morphometric analyses could not been taken on the cranium ULg PA BR-II-81-146; these were coded as missing values (NA). *Panthera gombaszoegensis* shows some typical pantherine morphological characters such as a robust cranium, a well-developed sagittal crest, a marked nuchal crest (Mazák *et al.* 2011), and a frontoparietal suture located close to the postorbital constriction (Christiansen 2008). The ULg PA BR-II-81-146 cranium is slightly larger than a living leopard (*P. pardus*), jaguar (*P. onca*) or a snow leopard (*P. uncia*) but relatively smaller than the two largest extant species: the tiger (*P. tigris*) and the lion (*P. leo*) in terms of cranial length. The mandibular material from ‘La Belle Roche’ (Fig. 2C–E) consisted of three fragments: the first fragment (ULg-PA-BR-III-M13-79), is as fragment of right dentary with an extremely worn canine, but with a well preserved p3 and m1 (Fig. 2C). The second mandibular (ULg-PA-BRII-455) is a left dentary with a worn canine, fairly well preserved p3 and p4, but extremely damaged m1 (Fig. 2D). The last fragment (ULg-PA-20210823-01) completely misses the lower canine, but has a complete p3, p4 and an almost complete m1 which is only lacking the protocone (Fig.2E). All ULg-PA-20210823-01 cheek teeth have been worn to some extent.

Dorsal view

The morphology and layout of fronto-nasal and fronto-maxillary sutures are often cited as good criteria for distinguishing between pantherines (e.g. Boule 1906). Those sutures are slightly discernible in *P. gombaszoegensis* from ‘La Belle Roche’ and appear to extend to approximately the same level, comparable to *P. leo* or *P. onca* (Fig. 4, no. 1). In all the pantherines examined, the fronto-nasal suture extends posteriorly to the posterior fronto-maxillary suture, except in *P. uncia*. In dorsal view the length and width of the snout varies in our dataset (Fig. 4, nos. 2 and 3).

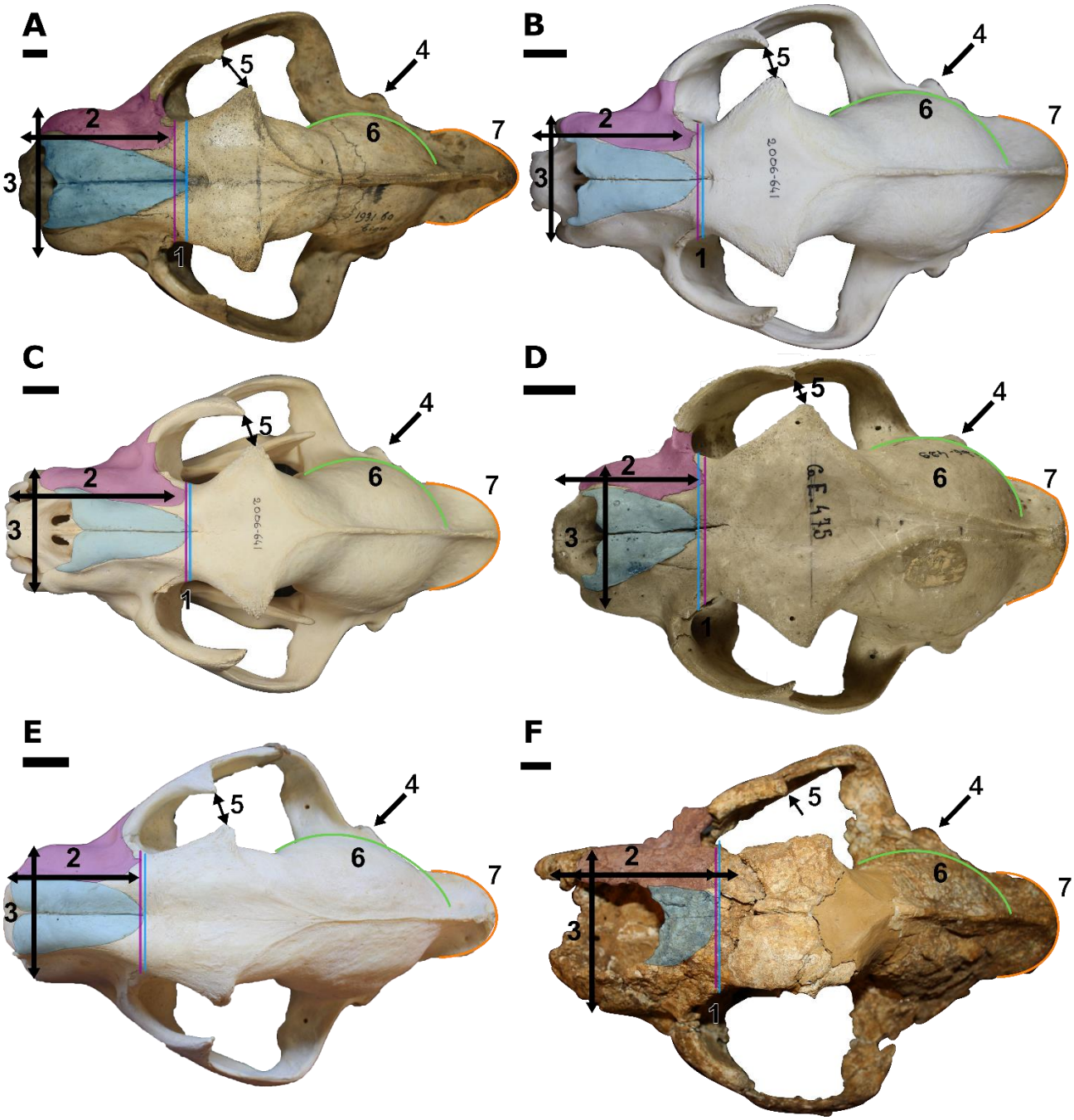

***Figure 4**: Crania of the different pantherines used for comparison in dorsal view. **A** P. tigris MNHN-ZM-AC-1931-60, **B** P. onca MNHN-ZM 2006-641, **C** P. leo RMCA-34836, **D** P. uncia MNHN-ZO-AC 1917-18, **E** P. pardus RMCA-29292, **F** P. gombaszoegensis ULg PA BR-II-81-146. Scale bars represent 2cm. 1, posterior extent of fronto-nasal and fronto-maxillary sutures; 2, snout length; 3, snout width; 4, mastoid process; 5, postorbital process of frontal; 6, curvature of braincase; 7, occipital shape.*

It is least elongate and broadest in *P. tigris,* with the length increasing and width decreasing through modern pantherines in a generally size-associated pattern from *P. leo*, to *P. onca,* to *P. pardus*, and finally to *P. uncia*. The snout morphology of *P. gombaszoegensis* fits the pattern, falling between that of the lion (*P. leo*) and jaguar (*P. onca*). In addition, the snout of *P. gombaszoegensis* is wide and straight, it does not appear constricted as in *P. tigris,* as has been described by previous authors (Jiangzuo & Liu 2020). The mastoid processes protrude slightly in dorsal view (Fig. 4, no. 4), more so than in *P. uncia* or *P. pardus,* with similarities to the larger modern species *P. leo* and *P. tigris*. The post-orbital region is of a similar relative size in all pantherines described except in *P. uncia*, in which it is incredibly large. The post-orbital process of the frontal of *P. gombaszoegensis* (Fig. 4, no. 5) is only moderately developed, as in the extant pantherines except for *P. uncia,* where it is more prominent. The post-orbital process of the zygomatic of ULg PA BR-II-81-146 is badly damaged on the left side, but is fairly well preserved on the right side and appears more developed compared to modern pantherines. A considerable portion of the frontal region has been altered; however, as best as can be determined, it was originally slightly depressed as observed in *P. onca* and *P. tigris* rather than flat as in *P. leo*, *P. atrox* (Merriam 1909; Martin & Gilbert 1978) and *P. spelaea* (Martin & Gilbert 1978). The braincase appears less rounded than in most of the extant pantherines, except for *P. tigris* (Fig. 4, no. 6). The occipital is moderately developed (Fig. 4, no. 7) and rather rounded; this is most similar to the condition of *P. leo* within living felines. The zygomatic arch has been deformed, but it appears relatively wide. The partial cranium CHA.100-f.8-73 from Château Breccia, which still has the left zygomatic arch in its original state and position, seems to confirm this assertion (see Plate 1 Argant & Argant 2011). The *P. gombaszoegensis* cranium from Château Breccia also possess zygomatic arches which are more triangular in shape, thus appearing more similar to larger modern pantherines (*P. tigris* and *P. leo*).

Lateral view

In lateral view, the braincase appears less rounded than is usually observed in mid-sized pantherine species (Fig. 5, no. 1) (e.g. *P. onca*, *P. uncia*, *P. pardus*) with a narrow intertemporal region, more comparable to the larger species *P. tigris* and *P. leo*. In P*. pardus and P. onca*, the dorsal profile tends to form less pronounced curve from the nasal aperture to the sagittal crest (Fig. 5, no. 2), whereas there is an abrupt angle between the nasal and the frontal region in both *P. tigris* and *P. gombaszoegensis*. This is more pronounced than in *P. leo*, although this feature remains most pronounced in *P. uncia*. Previous work also noted a similarly slight angle between those two planes in the American lion *P. atrox*, comparable to modern lions (*P. leo*) (Merriam 1909). The nuchal crest (Fig. 5, no. 3) is slightly prominent in lateral view, much less so than in *P. tigris* but still more pronounced than in *P. onca*.

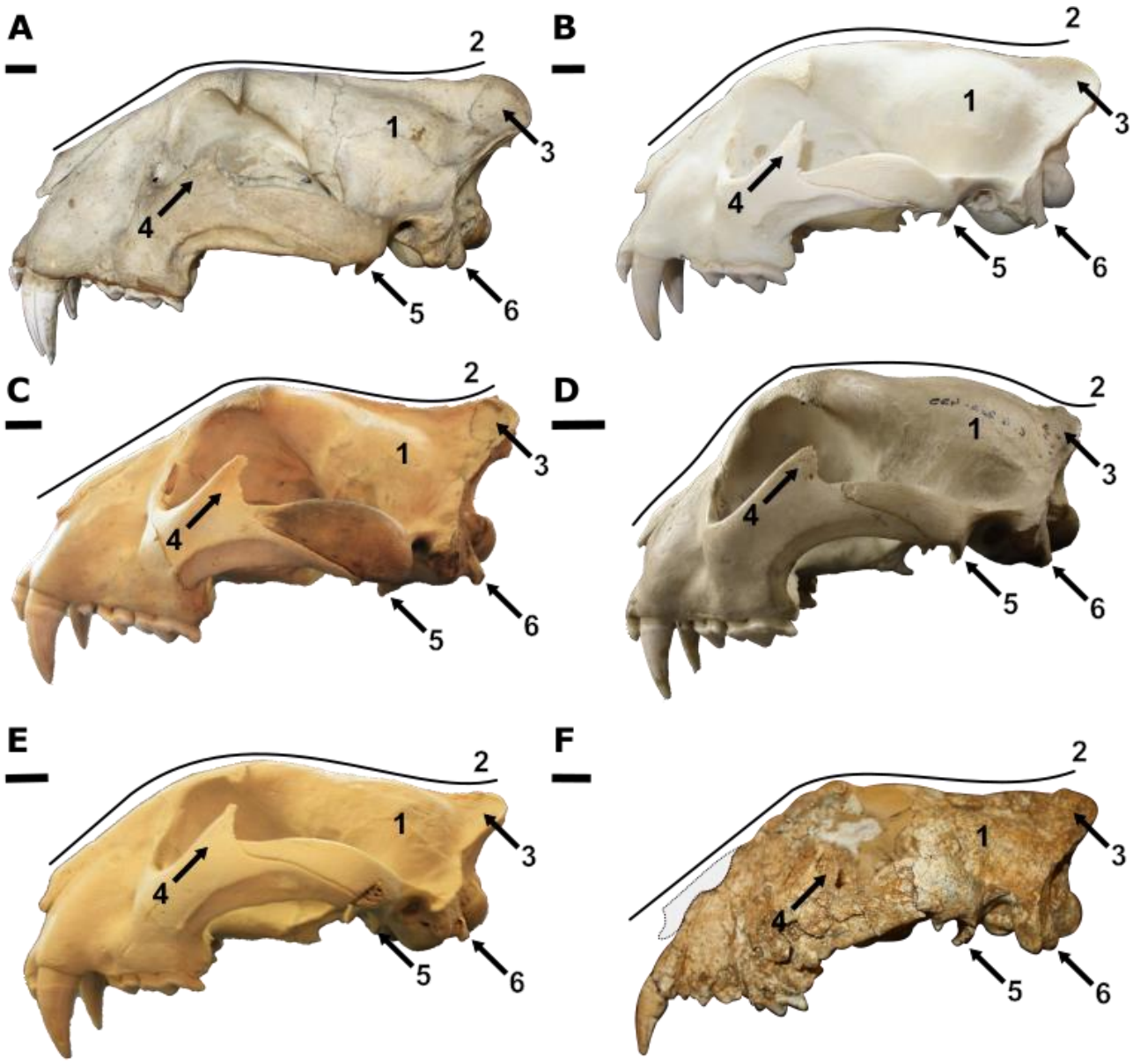

Figure 5*: Crania of the different pantherines used for comparison in lateral view.* ***A*** P. tigris *MNHN-ZM-AC-1931-60,* ***B*** P. onca *MNHN-ZM 2006-641,* ***C*** P. leo *RMCA-34836,* ***D*** P. uncia *MNHN-ZO-AC 1917-18,* ***E*** P. pardus *RMCA-29292,* ***F*** P. gombaszoegensis *ULg PA BR-II-81-146. Scale bars represent 2cm. 1, shape of the braincase; 2, dorsal profile shape; 3, nuchal crest profile; 4, postorbital process of the zygomatic; 5, post-glenoid process; 6, jugular process.*

Also, the postorbital process of the zygomatic is wider than in *P. onca* (Fig. 5, no. 4), and more similar to those of larger pantherine species. The postorbital process of the frontal of ULg PA BR-II-81-146 is completely missing on the left side and broken on the right side. Nevertheless, from its base it is clearly thicker than in *P. uncia* or *P. pardus*, but thinner than in the two largest extant species *P. leo* or *P. tigris*, ultimately being most similar to *P. onca*. The post-glenoid

process (Fig. 5, no. 5) is relatively large and easily discernible in lateral view. The jugular process (Fig. 5, no. 6) is ventrally directed, contrary to that observed for *P. uncia* and *P. pardus* where it is more posteriorly projected. The posterior face of the zygomatic arch is inclined, as in all the other pantherines.

Ventral view

The basicranial area of ULg PA BR-II-81-146 is quite well preserved and shows a clearly discernible opening of the oval foramen in ventral view (Fig. 6, no. 1), comparable to those of *P*. *onca*. The foramen is located at the level of the glenoid fossa, opening anterio-laterally as in other pantherines. This foramen is similar both in terms of size and shape to those of all pantherines, extant or fossil (see figures in Martin & Gilbert (1978); Sotnikova & Nikolskiy (2006); Christiansen & Harris (2009)), with the exception of the Miocene-Pliocene '*P.' blythae,* where this foramen appears more developed than in more recent taxa (see Fig. 1 in Tseng *et al.* (2013)). In ventral view the choanae opens slightly posterior to the postorbital process of the zygomatic (Fig. 6, no. 2); this arrangement is particularly uncommon in pantherines: in *P. leo* it is approximately at the level of the postorbital process of the zygomatic, whereas it clearly extends anterior to this process in all other pantherines except for the jaguar (*P. onca*) and the snow leopoard (*P. unica*), which exhibit a condition extremely similar to *P. gombaszoegensis.* For fossil pantherines, previous studies indicate that the choanae of *P. spelaea* extends slightly posterior to the postorbital process of the zygomatic (see Fig. 2 in Sotnikova & Nikolskiy (2006)), with the opposite being true for '*P.' blythae* (anterior to the process; see Fig. 1 in Tseng *et al.* (2013)). The region between the auditory bullae (Fig. 6, no. 3) of *P. gombaszoegensis* is flat and wider than in modern large-size pantherines, which is also the case for the cranium from Château Breccia (Argant & Argant 2011). In *P. tigris* and *P. onca* the occipital condyles extend on the ventral part of the cranium and join but this is not the case in other extant pantherines (Fig. 6, no. 4). The junction between the condyles projects anteriorly in *P. tigris* and *P. onca*, but is even more anteriorly protruded in *P. gombaszoegensis.* The jugular process (Fig. 6, no. 5) is well marked in *P. gombaszoegensis*, falling between the morphology of *P. tigris* and that of *P. onca*. The external occipital protuberance (Fig. 6, no. 6) is well pronounced, but the supraoccipital bone is almost invisible in ventral view. In extant pantherines, this condition is observed in *P. leo, P. pardus,* and *P. uncia*, although both *P. pardus* and *P. tigris* have a much more pronounced external occipital protuberance than *P. gombaszoegensis.* The palatine is relatively wide in *P. gombaszoegensis*, and its shape resembles that of *P. uncia* and *P. onca*. However, the palate appears quite large; this represents one of the main differences between *P. gombaszoegensis* and *P. onca*, as noted by Argant and Argant (2011).

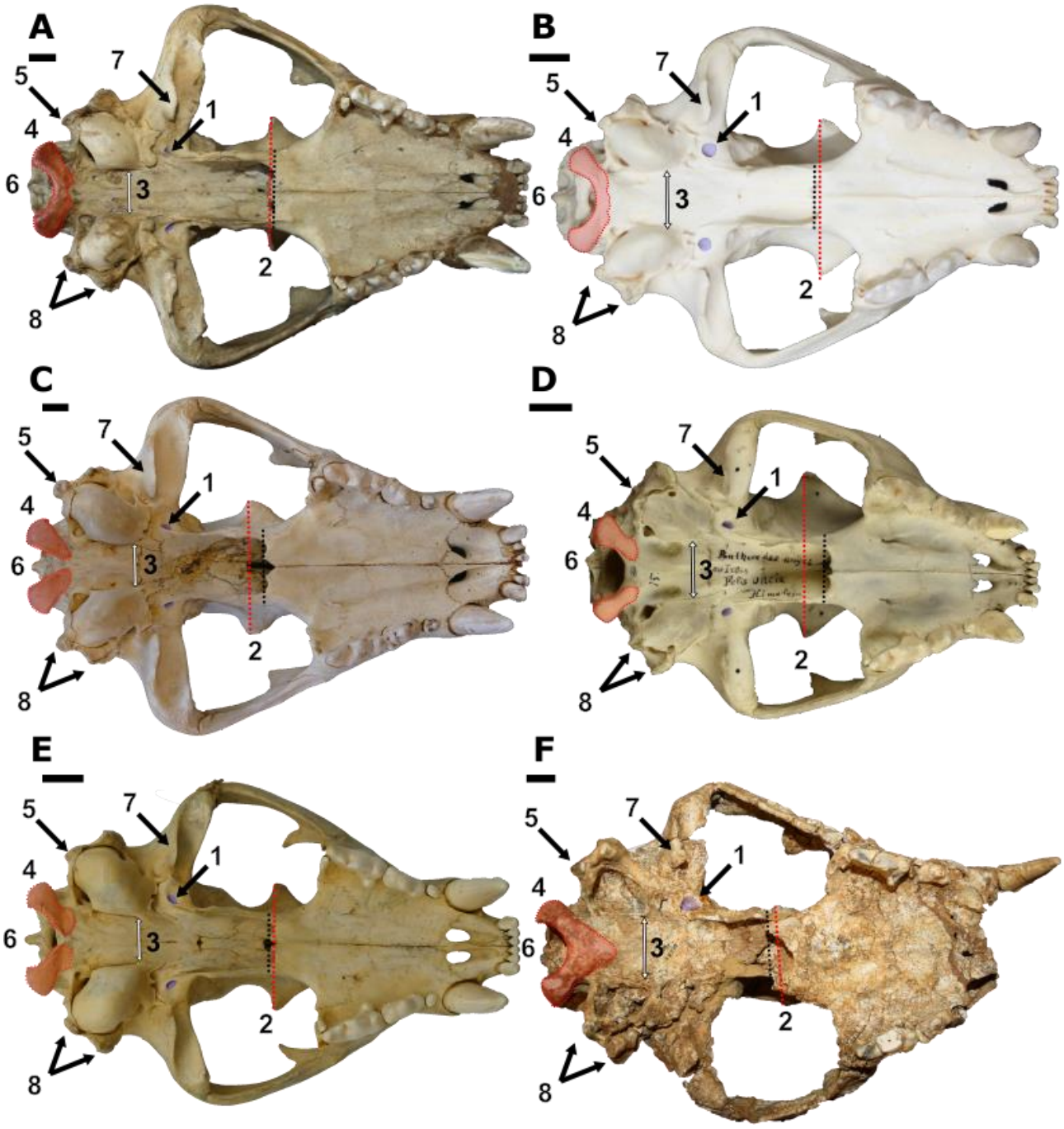

Figure 6: *Crania of the different pantherines used for comparison in ventral view.* ***A*** *P. tigris MNHN-ZM-AC-1931-60,* ***B*** *P. onca MNHN-ZM 2006-641,* ***C*** *P. leo RMCA-34836,* ***D*** *P. uncia MNHN-ZO-AC 1917-18,* ***E*** *P. pardus RMCA-29292,* ***F*** *P. gombaszoegensis ULg PA BR-II-81-146. Scale bars represent 2cm. 1, opening of the oval foramen; 2, postorbital process of the zygomatic; 3, region between the auditory bullae; 4, occipital condyles extend on the ventral part of the cranium; 5, jugular process; 6, external occipital protuberance; 7, post-glenoid process; 8, shape of the mastoid process and the jugular process.*

The post-glenoid process (Fig. 6, no. 7) is of moderate size, similar to *P. tigris and P. onca*, and more developed than in *P. leo*, *P. pardus* and *P. uncia*. The shape of the mastoid process and the jugular process (Fig. 6, no. 8) greatly resemble those of *P. tigris*, *P. onca* and *P. uncia* in ventral view; the jugular process is less developed than in *P. leo* but more so than *P. pardus*, whereas the mastoid process is much more developed than in *P. leo* and protrudes slightly more than in *P. pardus* or *P. uncia*.

Posterior view

The nuchal ridge of *P. gombaszoegensis* is relatively thick (Fig. 7, no. 1) and high relative to smaller pantherines (e.g. *P. pardus*; *P. onca*), comparable to *P. leo*. The occipital condyles (Fig .7, no. 2) appear larger than in any extant pantherine (except for *P. uncia*), and also larger than in *P. atrox* (Figure 1 Merriam 1909) or in *P. spelaea* (Figure 2 and Figure 3 Sotnikova & Nikolskiy 2006). In posterior view, the zygomatic arches appear relatively wider than in *P. onca*, *P. uncia, P. leo* or *P. pardus* and more comparable to *P. tigris*. The intercondyloid notch is concave, similar to *P. tigris, P. pardus, P. uncia* or *P. onca*. The notch appears more deeply concave in *P. leo.* The gap between both occipital condyles (Fig. 7, no. 3) is moderately wide, comparable to that of *P. tigris*, *P. onca* and *P. uncia*, much wider than in *P. leo*, but narrower than in *P. pardus*. In posterior view the dorsal line of the *P. gombaszoegensis* appears slightly concave (Fig. 7, no. 4), more than in *P. onca and P. pardus*. It is similar to that observed in *P. tigris*. Yet this concavity is still much less pronounced than the condition in *P. leo* or *P. uncia*. The condyloid fossa (Fig. 7, no. 5) is marked and reassembles that of *P. onca*. It is somewhat less marked than in *P. tigris* and *P. uncia*, but more pronounced than those of the other pantherines studied. Both paracondylar process are missing. The largest extant pantherines (*P. tigris* and *P. leo*) exhibit a process above the supraoccipital bone, separated from the nuchal crest (Fig. 7, no. 6). This process seems to be present but is much smaller and closer to the nuchal crest in *P. onca*, whereas this process is completely absent in *P. gombaszoegensis*, reassembling the condition in the cranium of *P. pardus*.

Anterior view

In anterior view (Fig. S5) the zygomatic arches and the snout of *P. gombaszoegensis* appear wide. In particular, the snout of *P. gombaszoegensis* wide such that it obscures the infraorbital foramen, as in *P. tigris*. The infraorbital foramen is similar in terms of size and shape to the other pantherines. The lacrimal process is absent, or at least extremely reduced, as in *P. pardus*; this process is present and well developed in all other extant pantherines.

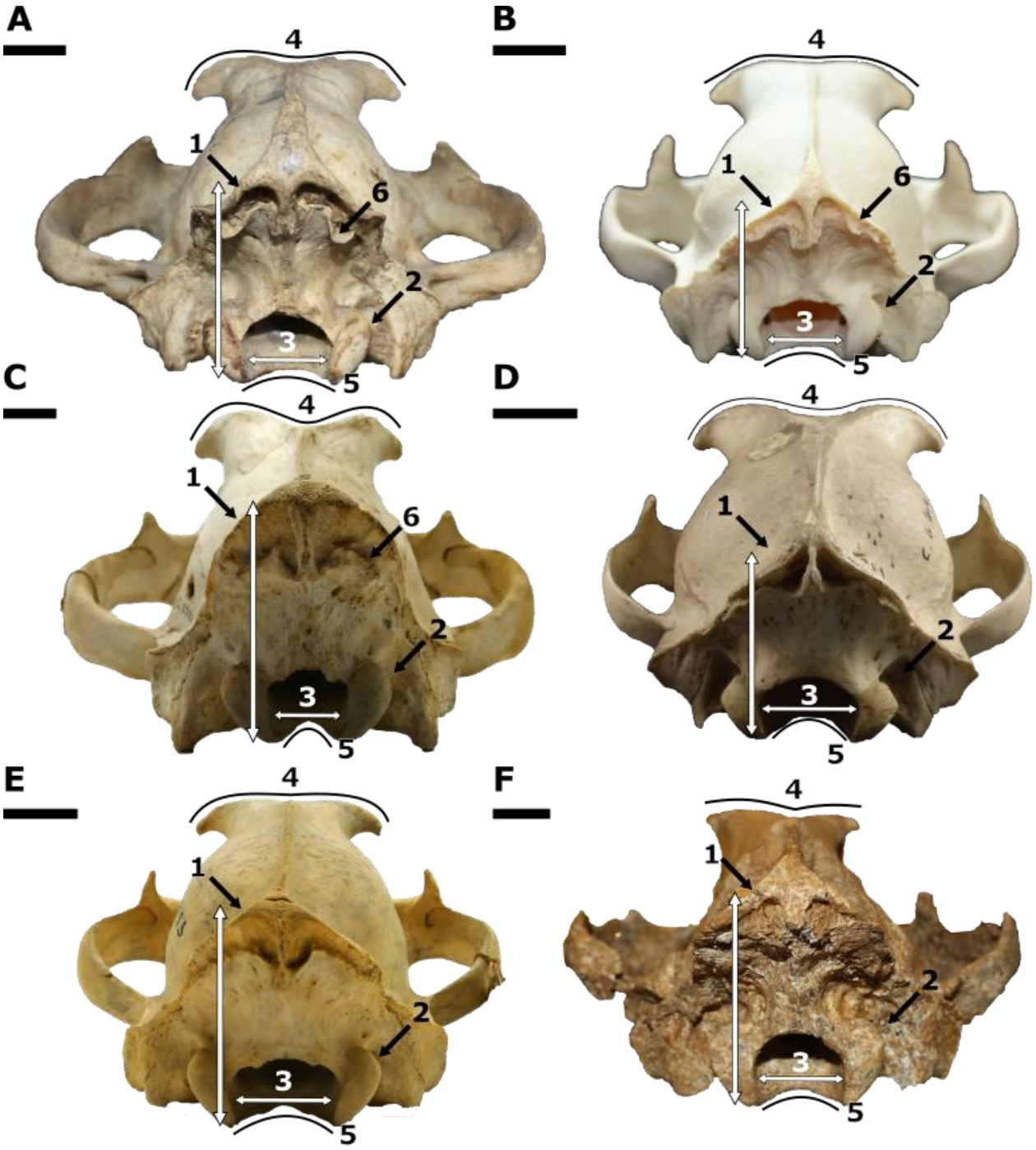

Figure 7: *Crania of the different pantherines used for comparison in posterior view.* ***A*** *P. tigris MNHN-ZM-AC-1931-60,* ***B*** *P. onca MNHN-ZM 2006-641,* ***C*** *P. leo RMCA-34836,* ***D*** *P. uncia MNHN-ZO-AC 1917-18,* ***E*** *P. pardus RMCA-29292,* ***F*** *P. gombaszoegensis ULg PA BR-II-81-146. Scale bars represent 2cm. 1, nuchal ridge; 2; occipital condyles 3, gap between both occipital condyles; 4, dorsal line of the cranium; 5, condyloid fossa; 6, process above the supraoccipital bone.*

Upper dentition

Contrary to cranial traits, an extensive and well-documented comparative description of the dentition of *P. gombaszoegensis* has already been published (Jiangzuo & Liu 2020). Therefore, in this section we will focus on dental traits of the ULg-PA-BR-II-81-146 *P. gombaszoegensis* specimen which vary from previous descriptions, and highlight notable dental features of the specimen. Jiangzuo & Liu (2020) noted that upper dentition of *P. gombaszoegensis* differs mainly from that of *P. onca* by way of well-defined vertical grooves of the canine and less robust premolars (especially P3). In our sampling, the vertical groove is absent or indiscernible on the canine of ULg-PA-BR-II-81-146 from 'La Belle-Roche', and it is extremely reduced in the *P. onca* specimens we examined, whereas it is clearly present in the other pantherines. Thus, the presence of such a groove appears variable in *P. gombaszoegensis*, exactly as in *P. onca* (Seymour, 1989). Also, in our dataset, the P3 of *P. gombaszoegensis* appears more robust than in *P. onca* or *P. pardus,* but less so than in the other taxa, differing from previous descriptions (Jiangzuo & Liu 2020). Moreover, according to Jiangzuo & Liu (2020), the upper dentition of *P. gombaszoegensis* also differs from the lineages of *P. leo* and *P. spelaea* in several points, in particular a smaller and less marked anterior accessory cusps of P3. The third upper premolar of the specimen from 'La Belle-Roche' is damaged, but we can see that the anterior accessory cusp is undeniably extremely reduced (maybe the most reduced in our dataset with the exception of the living tiger, *P. tigris*). On the P3 of *P. gombaszoegensis*, the posterior cusp is large with a marked cingulum, but less clear than in extant pantherines.

Panthera gombaszoegensis ULg-PA-BR-II-81-146 also exhibits a well-developed P4 protocone, being less robust than in *P. leo*. The specimen from la Belle-Roche also seems to lack a well-defined ectoparastyle on the P4.

Results

Phylogenetic relationships of pantherines

A single most parsimonious tree was recovered in all analyses (Fig. 8A). These trees have a length of: 11.7 for K=3, 7.05952 for K=6, 5.06364 for K=9 and 3.94945 for K=12. As recently suggested by Goloboff, Torres, & Arias (2017), better results are obtained with a weaker concavity. Most of the taxa in our analysis were constrained based on the results of molecular analyses except for three fossil taxa: *P. gombaszoegensis, P. palaeosinensis* and '*P.*' *blythae.* In the phylogenetic tree obtained through Bayesian inferences on a combined morphological and molecular dataset published by Tseng *et al.* (2013) , *P. palaeosinensis* was recovered at the base of the Pantherinae, whereas in our topology it clusters with *N. nebulosa* which is not considered as a pantherine.

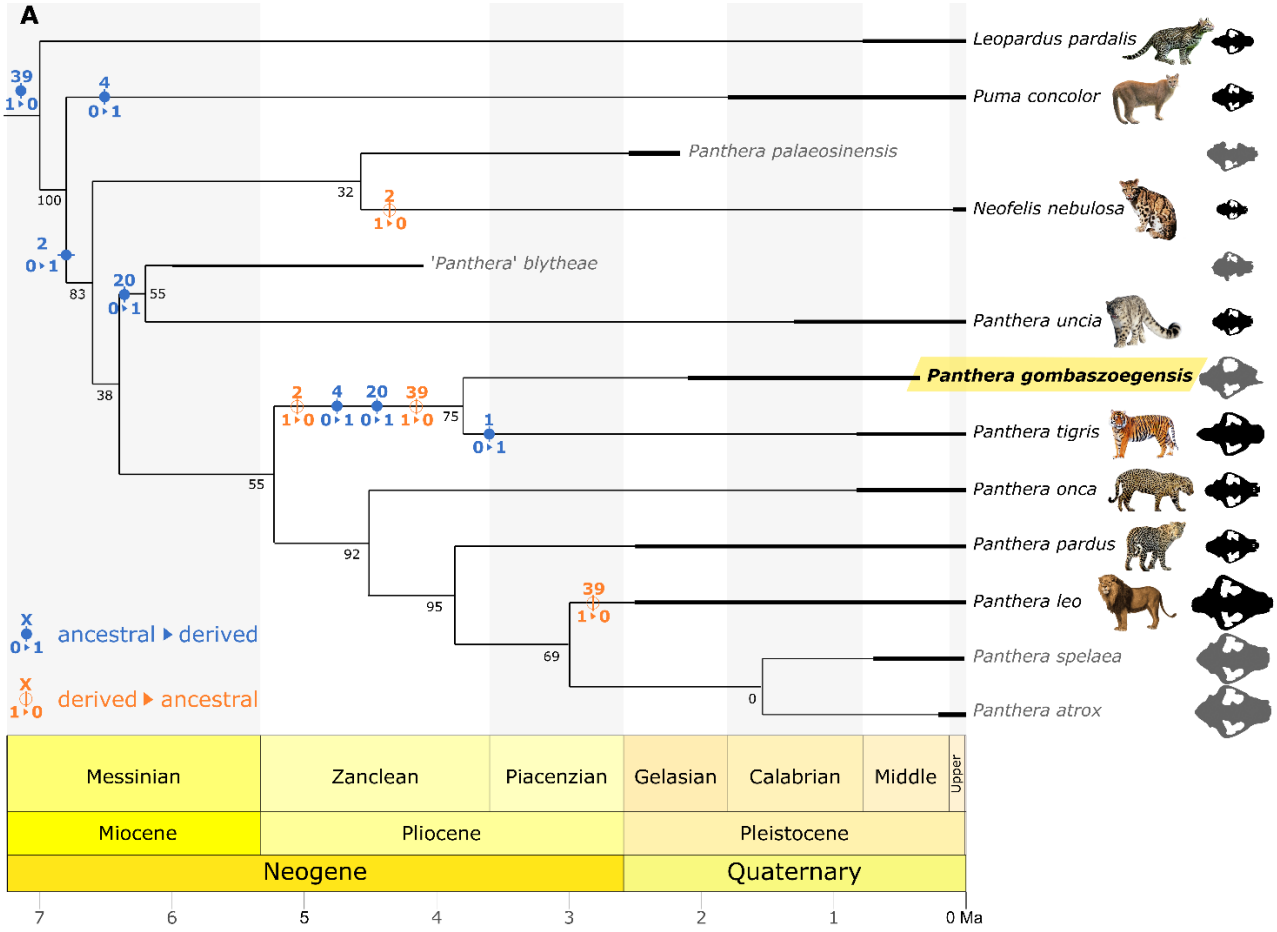
A
Leopardus pardalis
Puma concolor
Panthera palaeosinensis
Neofelis nebulosa
'Panthera' blytheae
Panthera uncia
Panthera gombaszoegensis
Panthera tigris
Panthera onca
Panthera pardus
Panthera leo
Panthera spelaea
Panthera atrox
ancestral ▸ derived
derived ▸ ancestral
Messinian
Zanclean
Piacenzian
Gelasian
Calabrian
Middle
Upper
Miocene
Pliocene
Pleistocene
Neogene
Quaternary
7
6
5
4
3
2
1
0 Ma

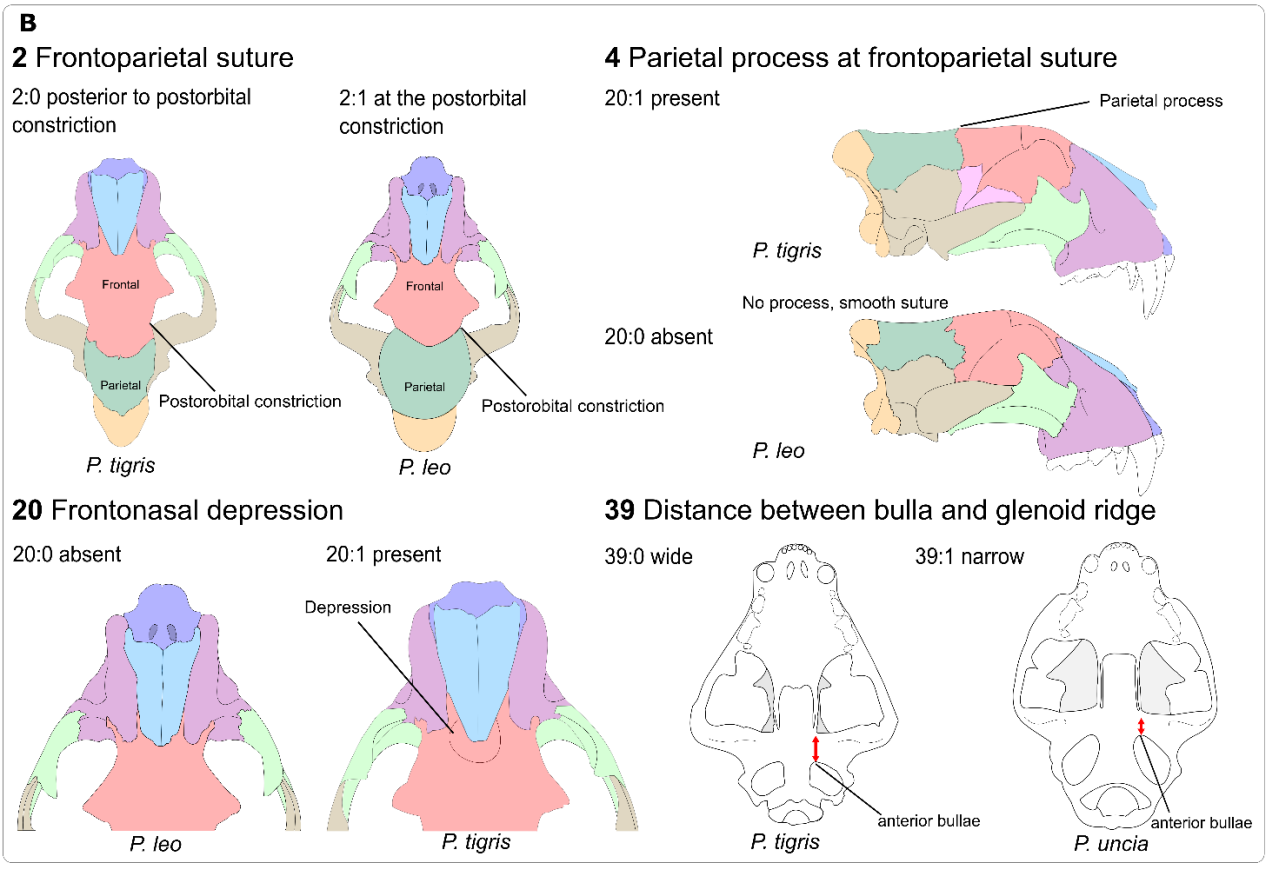
B
2 Frontoparietal suture
2:0 posterior to postorbital constriction
2:1 at the postorbital constriction
Frontal
Parietal
Postorbital constriction
P. tigris
P. leo
4 Parietal process at frontoparietal suture
20:1 present
Parietal process
P. tigris
20:0 absent
No process, smooth suture
P. leo
20 Frontonasal depression
20:0 absent
20:1 present
Depression
P. leo
P. tigris
39 Distance between bulla and glenoid ridge
39:0 wide
39:1 narrow
anterior bullae
P. tigris
anterior bullae
P. uncia

***Figure 8**: **A** Single most parsimonious tree arising from implied weighting (k=12, see Appendix S1 for the script) analysis of the character matrix (Morphobank project P4265). Fossil taxa are represented in grey. **B** Illustrations of the synapomorphies uniting P. gombaszoegensis and P. tigris.*

However, the node uniting *P. palaeosinensis* and *N. nebulosa* present a low symmetric resampling value (32), despite these two taxa being united by two synapomorphies: an intermediate nasal width at aperture (character 14:1), and a mandible depth anterior to p3 that is deeper than the depth at p4/m1 (character 44:1). In our analysis, and as in Tseng *et al.* (2013), '*P.' blythae* forms a clade with *P. uncia* which is supported by a symmetric resampling value of 55.

The most interesting result of our phylogenetic analyses is that *P. gombaszoegensis* is systematically recovered as closer to *P. tigris* than to *P. onca*, no matter the importance of homoplastic characters. The *P. gombaszoegensis* + *P. tigris* clade is supported by four unambiguous but homoplastic synapomorphies: a frontoparietal suture posterior to the postorbital constriction (character 2:0), the presence of a parietal process at the dorsal frontoparietal suture (character 4:1), and the presence of a frontonasal depression (character 20:1) and a wide distance between the anterior bullae and the glenoid ridge (character 39:0) (Fig. 8B). This node is also well supported by a high symmetric resampling value of 75 (Fig. 8A). All those synapomorphies of the *P. gombaszoegensis* + *P. trigis* being homoplastic they are found in other taxa, the frontoparietal suture posterior to the postorbital constriction (character 2:0) is also seen in *N. nebulosa.* The presence of a parietal process at the dorsal frontoparietal suture (character 4:1) is also observed in the mountain lion, *Puma concolor.* The presence of a frontonasal depression (character 20:1) is shared with the *P. uncia* - '*P*.' *blytheae* clade and finally the wide distance between the anterior bullae and the glenoid ridge (character 39:0) is also observed in *P. leo*. This very last character states might be influenced by allometry as states 0 was observed in the three largest species (*P*. *gombaszoegensis*, *P. tigris*, *P. leo*) but a larger dataset of large taxon and some correlations would be needed to test this hypothesis.

Multivariate morphometric analysis: upper dentition

A first two-dimensional morphospace was retrieved using a Principal Coordinates Analysis (PCoA) (Fig. 9A). This PCoA retrieved 19 axes (Fig. S6A), with the two first axes explaining 22.44% and 5.55% of variance respectively. The first axis is mainly influenced by the aspect ratio of the canine (CH/CL), the length of P3 (P3L/CL) and both measurements taken on the P4 (P4L/ CL and P4W/ CL), whereas the second axis is more influenced by the canine width (CW/CL) and the P3 width.

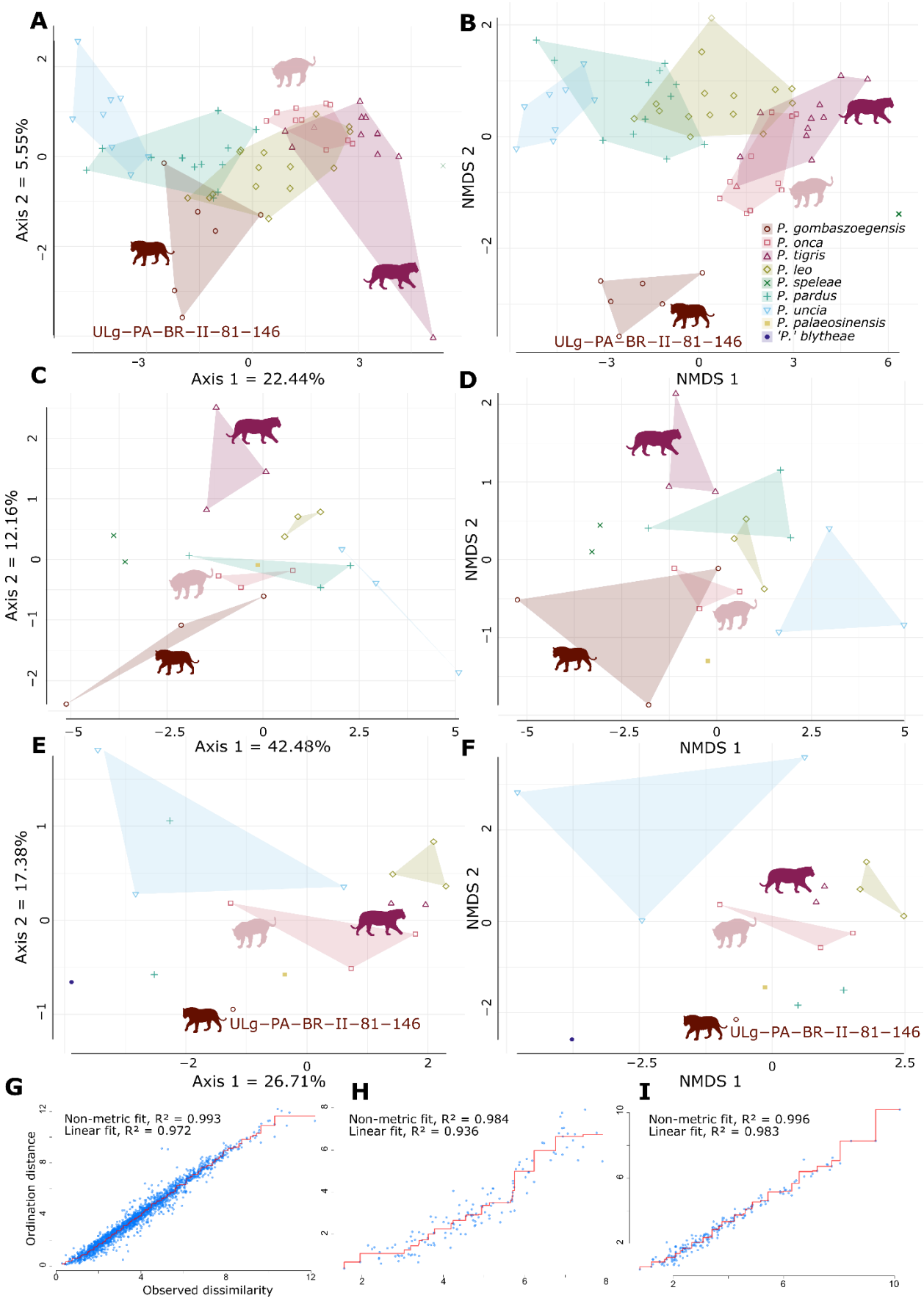
A
B
C
D
E
F
G
H
I
Axis 2 = 5.55%
Axis 1 = 22.44%
NMDS 2
NMDS 1
Axis 2 = 12.16%
Axis 1 = 42.48%
Axis 2 = 17.38%
Axis 1 = 26.71%
ULg−PA−BR−II−81−146
P. gombaszoegensis
P. onca
P. tigris
P. leo
P. speleae
P. pardus
P. uncia
P. palaeosinensis
'P.' blytheae
Ordination distance
Observed dissimilarity
Non-metric fit, R² = 0.993
Linear fit, R² = 0.972
Non-metric fit, R² = 0.984
Linear fit, R² = 0.936
Non-metric fit, R² = 0.996
Linear fit, R² = 0.983

*Figure 9: Results of the multivariate morphometric analyses. **A**, PCoA on the upper dentition dataset; **B**, NMDS on the upper dentition dataset; **C**, PCoA on the lower dentition dataset; **D**, NMDS on the lower dentition dataset; **E**, PCoA on the cranium dataset; **F**, NMDS on the cranium dataset; **G**, non-metric fit of the two-dimensional NMDS on the original dissimilarities for the upper dentition dataset (k = 2; stress = 0.08330135); **H**, non-metric fit of the two-dimensional NMDS on the original dissimilarities for the lower dentition dataset (k = 2; stress = 0.03082973); **I**, non-metric fit of the two-dimensional NMDS on the original dissimilarities for the cranium dataset (k = 2; stress = 0.1256406). Animal silhouettes were obtained from PhyloPic (phylopic.org). Image credits: Manabu Sakamoto (P. onca) and Sarah Werning (P. tigris).*

While all pantherines specimens are well spread on the first axis, they strongly overlap on the second with only a few *P. gombaszoegensis* and one *P. tigris* specimens occupying the lowest portion of the axis and *P. uncia* showing the highest PC values. At first sight Axis 1 might seem to be well sorted by size; however, *P. gombaszoegensis* occupy much lower values than *P. onca* while being larger. *Panthera onca* overlap *P. leo* in the morphospace while *P. pardus,* which is supposed to be part of the 'lion group' in our phylogeny is closer to *P. uncia.*

The closest taxa to *P. gombaszoegensis* on the first axis are *P. pardus* and *P. leo* specimens. PERMANOVA retrieved a significant difference between *P. onca* and *P. gombaszoegensis* in terms of upper dentition proportions, with a p-value of 0.001 (FDR-corrected, $p \leq 0.003$). However, according to our PERMANOVA results *P. gombaszoegensis* differs from any of the extant pantherines in terms of dental proportions (*P. tigris* 0.002, FDR-corrected $p \leq 0.001$; *P. pardus* 0.001, FDR-corrected $p \leq 0.001$; *P. leo* 0.001, FDR-corrected $p \leq 0.001$ and *P. uncia* 0.006, FDR-corrected $p \leq 0.001$).

The only taxa to exhibit similar values to *P. gombaszogensis* on Axis 2 is one specimen of *P. tigris* which could be explained by their phylogenetic affinities that we highlighted previously but may also be explained by intraspecific variation. The Pagel´s Lambda for the first axis was close to zero showing there is no phylogenetic signal on this axis (Table 1).

Table 1: Results obtained with the phylosig function in each dataset.

	Pagel´s Lambda	logL Lambda	p-value	Phylogenetic signal
Lower dentition	6.6107e-05	-11.7486	1	None
Upper dentition	6.6107e-05	-11.0724	1	None
Cranium	6.6107e-05	-6.31618	1	None

A second two-dimensional morphospace was performed using a non-metric multidimensional (NMDS) (Fig. 9B). In the NMDS plot, *P. gombaszoegensis* clearly plots apart from other pantherine species. The pantherine taxa occupy a wide range of values on the NMDS1 while they are confined to values between -1 and 2 on the second, the only exception being *P. gombaszoegensis* occupying the lower portion of the axis NMDS2. The non-metric fit of the two-dimensional NMDS on the original dissimilarities confirms that a two-dimensional plot represents the inter-specimen morphological distances very well (R^2 = 0.993 for k=2, stress value = 0.08330135) (Fig. 9G).

Multivariate morphometric analysis: lower dentition

Our PCoA computed on the 8 ratios from the lower dentition (Fig. 9C) retrieved 18 axes (Fig. S6B), with the first two PCo axes explaining 42.48% and 12.16% of variance respectively. The placement of specimens along the first axis is mainly influenced by measurements taken on the p3, p4 and m1 (p3l/cl, p3w/cl, p4l/cl, p4w/cl, m1w/cl and m1l/cl), whereas distribution across the second axis is mainly influenced by the check teeth length (ctl/cl) and the diastema length (diastema/cl). The three *P. gombaszoegensis* specimens included in this study are located in a region of morphospace with negative values on both axes, likely due to a high canine length compared to the measurements taken on the check teeth and the diastema. The closest species to *P. gombaszoegensis* in the morphospace are *P. onca* and *P. pardus* whereas the most dissimilar species are *P. tigris* and *P. uncia.* All the pantherines species are relatively occupies a relatively large part of the morphological space on the plot, except for *P. pardus* and *P. onca*. Interestingly, *P. spelaea* and *P. leo* are well separated from each other in the morphospace, with *P. spelaea* exhibiting negative values on the first axis while the modern lion shows positive values (yet values on the second axis are extremely similar). It should also be noted that the single specimen of *P. palaeosinensis* is comprised within the morphological space occupied by *P. pardus*. Resemblances between the lower dentition of *P. onca* and *P. gombaszoegensis* is corroborated using PERMANOVA, which did not retrieve any significant differences between those two taxa (p-value=0.4). PERMANOVA also did not retrieve any statistical difference between the lower dentition of *P. tigris* and *P. gombaszoegensis* (p-value=0.6), nor from *P. pardus* (p-value=0.1) but rather in *P. leo* (p-value=0.04) and *P. uncia* (p-value=0.01) although FDR corrections showed that those last two significant p-values were statistical artefActs (FDR-corrected $p \leq 0.1$ for *P. leo* and $p \leq 0.3$ for *P. uncia*). The Pagel´s Lambda for the first axis was close to zero showing there is no phylogenetic signal on this axis (Table 1).

The pattern observed from the NMDS plot (Fig. 9D) is somewhat similar, although there are still some differences worth mentioning: *P. onca* and *P.*

gombaszoegensis specimens almost completely overlap in the morphological space; *P. palaeosinensis* does not overlap with *P. pardus*; *P. spelaea* and *P. leo* are clearly separated from each other. The modern leopard (*P. pardus*) is clearly separated from *P. gombaszoegensis* in the morphospace, but the modern lion (*P. leo*) is relatively closer in this analysis. Again, the non-metric fit of the two-dimensional NMDS on the original dissimilarities shows a high R^2 of 0.996 for = 2, stress = 0.03082973 (Fig. 9H).

Multivariate morphometric analysis: cranium

The PCoA computed on the 12 cranial ratios (Fig. 9E) retrieved 15 axes (Fig. S6C), the first two explaining 26.71% and 17.38% of variance respectively. The first axis is mainly influenced by the post-orbital width (POW/COL), the braincase width (BrW/ COL), the palatal length (PaL/ COL), the basicranium length (BaL/COL) and the condylobasal width (CBW/COL) while the axis 2 is mostly influenced by the nasal width (NaW/COL), the mastoid process width (MaPW/COL), the orbital process length (OPL/COL) and the temporal fossa length (TFL/COL). Pantherines occupy a relatively large part of the morphological space on both PCo axes based on cranial ratios. *P. gombaszoegensis* is recovered close to *P. palaeosinensis* and '*P.*' *blythae* on the second axis of both the PCoA (Fig. 9E) and the NMDS2 (Fig. 9F). Cranial morphology of *P. gombaszoegensis* seems to be most removed from *P. uncia.* The Pagel´s Lambda for the first axis was close to zero showing there is no phylogenetic signal on this axis (Table 1). The pattern of morphospace occupation for the cranial dataset appears more similar between the PCoA and the NMDS than for the two previous datasets, although the non-metric fit of the two-dimensional NMDS on the original dissimilarities appears slightly lower than for the two previous datasets (R^2 = 0.984) (Fig. 9I).

Allometry

Our linear regressions between the cranial or canine length (upper and lower) and their respective scores on the first axis of the PCoA (Fig. S8-S10) show a clear allometric component in the features studied her, which is more marked (R^2_{adj} =0.82 for the upper dentition; R^2_{adj} = 0.84 for the lower dentition) for dental measurements than for the cranium (R^2_{adj} = 0.48). However, this trend is not retrieved in the other PCoA axes. Still, it is clear than *P. gombaszoegensis* show lower values on PCo axis 1 for the upper dentation dataset than similar sized *P. onca* specimens in our dataset. The allometric influence is present in the first PCo axis of our analyses, but is not prevalent in subsequent axes, with adjusted R^2 values dropping lower than 0.1 for PCo axes 2–10 in each morphometric dataset (Fig. S8–S10).

Discussion

Several authors have pointed out the resemblances between *P. onca* and *P. gombaszoegensis* (e.g. Argant & Argant 2011; Marciszak 2014; Stimpson *et al.* 2015; Jiangzuo & Liu 2020), leading to the characterisation of the latter as the 'European jaguar' or 'Eurasian jaguar' (e.g. Argant and Argant 2011; Hemmer *et al*. 2001; Jiangzuo and Liu 2020; Marciszak and Lipecki 2021; Mol e*t al*. 2011; Stimpson *et al*. 2015). Bonifay (1971) mentioned its resemblance to *P. leo*, and other felids, based on cranial fragments and upper teeth of young adults. Then, O'Regan (2002) noted that it was more similar to the modern tiger (*P. tigris*) and jaguar (*P. onca*) than to any extant or extinct lion (*P. leo, P. spelaea, P. atrox*) or leopard (*P. pardus*). Later, its resemblances with the modern tiger were forgotten as authors assigned it as a subspecies of *P. onca* (Hemmer *et al.* 2001, 2010; Hankó 2007; Mol *et al.* 2011); more recent works regard *P. gombaszoegensis* as a valid species in its own right (e.g. Argant & Argant 2011; Reynolds 2013; Marciszak 2014; Stimpson *et al.* 2015; Jiangzuo & Liu 2020), yet its phylogenetic affinity is often still considered close to *P. onca*. Our implied weighting analysis retrieved *P. gombaszoegensis* to be phylogenetically closer to *P. tigris* than to *P. onca*. This relationship is supported by four synapomorphies and a strong symmetric resampling value (Fig. 8A). Many authors stretch the fossil record of the tiger back to about 2 myr, some even considering *P. palaeosinensis* as a subspecies of *P. tigris* (*P. tigris palaeosinensis*) (Hemmer 1968*a*, *b*; Groves 1992; Yiqing & Yan 2010; Mazák *et al.* 2011), thus implying an Asian origin for the tiger lineage. Kitchener and Yamaguchi (2010) suggested it may have been a primitive taxon that gave rise to modern tigers, lions, leopards, and jaguars. Our analysis (and that of Tseng *et al*. (2013)) retrieved *P. palaeosinensis* as a basal pantherine, with our topology placing this taxa outside of crown *Panthera* and as sister to *Neofelis* (Fig. 8A). Our analyses recognise the presence of a stem tiger (*P. gombaszoegensis*) in the Pleistocene of Europe which contradicts the previous hypotheses concerning the origin of *P. tigris*. *Panthera gombaszoegensis* was theorised to have migrated to North America from eastern Asia during the Early Pleistocene through Beringia, following different potential dispersal scenarios (Kurtén 1973; Argant & Argant 2011; Jiangzuo & Liu 2020). However, the affinities between *P. gombaszoegensis* and *P. onca* has always been unclear, especially given that *P. onca* is endemic to the American continent (Seymour 1989), with its first uncontested fossil remains being found in the Hamilton Cave (West Virginia) dating from 820-850 kya (Repenning *et al.* 1995). Yet, *P. gombaszoegensis* has never been identified on the American continent, nor even in eastern Asia. The first fossil that can be clearly attributed to *P. tigris* is approximately 850 kyr old (Hemmer 1971), and according to different sources, the evolutionary origin of the modern tiger is presumably located in the north of China (Hemmer 1981,

1987; Mazák 1981; Herrington 1987). The Haro Quary river fauna (including some *P. gombaszoegensis* specimens) is estimated to be between 1.77 and 1.07 Myr old (Jiangzuo & Liu 2020), indicating that *P. gombaszoegensis* likely reached Asia just before the first *P. tigris* appeared. This is in accordance with the results of our phylogenetic analysis, and provides a more coherent scenario in terms of geographic dispersion through time (see Fig. 1a). Also, Jiangzuo & Liu (2020) already recognized that the specific assignments of some fossils to *P. gombaszoegensis* in eastern Asia was complex, due to the presence of a similar-sized pantherine (early *P. tigris*), clearly pointing towards an imbricated fossil record of *P*. *gombaszoegensis* and *P. tigris.*

P. gombaszoegensis was thought to be significantly larger than the extant jaguar (Argant & Argant 2011), but also smaller than most extant tigers (Jiangzuo & Liu 2020). Some living tiger subspecies are thought to significantly overlap *P. gombaszoegensis* when considered only dental size (e.g. *P. tigris sumatrae*, *P. tigris sondaica* or *P. tigris balica* see Mazák & Groves (2006)). As evolutionary allometry can affect bone shape, and thus influence the results of morphometrics analyses (Klingenberg 1996), and different studies have already highlighted the importance of considering evolutionary allometry when dealing with felids cranial shape and proportions (e.g. Slater & Van Valkenburgh 2009; Tamagnini, Meloro, & Cardini 2017), it may not be surprising that *P. gombaszoegensis* presents similarities with both the extant tiger (*P. tigris*) and the extant jaguar (*P. onca*) with regards to size, falling in between those two taxa. Nevertheless, we describe in this contribution a medium-sized specimen of *P. gombaszoegensis* (large female or small male) which varies in numerous features from *P. onca*. The differences we observe cannot be solely explained by allometric variation. Our morphospaces do not reflect the phylogeny we obtained (see Pagel´s Lambda and p-values in Table 1) which could mean that our ratios are more driven by ecological factors than by the phylogenetic relationships between our taxa. Key differences were revealed between the upper and lower dentition proportions for *P. gombaszoegensis*: our morphospaces corroborate the similarities in lower dentition between *P. gombaszoegensis* and *P. onca,* but these are not recovered for the upper teeth or for the cranium (though with only a single cranial specimen of *P. gombaszoegensis*). This discovery reiterates that dental characters should be treated carefully when dealing with taxa identification or phylogenetic reconstructions (especially those from the mandible), since morphological adaptations for feeding may obscure phylogenetic affinities (as discussed in Jernvall 2000; Jernvall & Jung 2000; Naylor & Adams 2001; Dávalos *et al.* 2014; Sansom *et al.* 2017; Billet & Bardin 2019). Indeed, the differences between upper and lower dentition observed in *P. gombaszoegensis* were already

discussed as an example of mosaic evolution within this taxon (Hemmer 1981). Despite occlusal surfaces of mammalian teeth supposedly corresponding perfectly, modularity is present within mammalian dentition Stock (2001), and other morphometric analysis already retrieved slightly different results for lower and upper dentition (e.g. Leroy *et al.* 2004; Bever 2005; Dumbá *et al.* 2022). Moreover, it seems that variations in dental proportions do not negatively affect the efficacy of occlusion (Ungar 2010).

The distinctiveness between the craniodental form of *P. gombaszoegensis* and *P. onca,* also has interesting palaeoecological implications. A number of authors have considered *P. gombaszoegensis* as a 'generalist' taxon (i.e. which would be able to hunt a wide spectrum of prey), certainly more so than *P. onca* (Jiangzuo & Liu 2020; Marciszak & Lipecki 2021) and comparable to the notably ubiquitous *P. pardus* (Marciszak 2014). The postcranial material available for *P. gombaszoegensis* has not recovered great similarities to *P. onca*. Indeed some similarities are clearly observable between these two taxa, but there is a large size difference and widespread resemblance with the post-crania of various pantherines (O'Regan 2002; Argant & Argant 2011). Argant & Argant (2011) insisted on the ability of *P. gombaszoegensis* to adapt to the harsh climates of glacial periods, as demonstrated by modern Siberian tigers (*Panthera tigris altaica*). However, *P. gombaszoegensis* has also often been described as an ecological equivalent of the modern jaguar, considered as a forest dweller with strong penchant for open water (Hemmer 1971; Hemmer *et al.* 2001). Marciszak and Lipecki (2021) suggested that, based on the observations published by Jiangzuo and Liu (2020), the moderately robust dentition of *P. gombaszoegensis* (compared to *P. onca*) would reflect its prey preferences. Marciszak and Lipecki (2021) also argued that the marked vertical grooves on the upper canines of *P. gombaszoegensis* and the poor development or even absence of this feature in *P. onca* are probably correlated with habitat and prey preference. However, we did not observe any significant variation in the robustness of the upper check teeth between *P. gombaszoegensis* and *P. onca*, and the vertical groove was not observed on the cranium of the *P. gombaszoegensis* ULg-PA-BR-II-81-146 specimen. This may be explained by intraspecific variation, and, if true, may further underline that those traits should not be used to infer any palaeoecological interpretations (and certainly not phylogenetic affinity). A wide prey spectrum could explain the presence of *P. gombaszoegensis* in various habitats (Marciszak and Lipecki 2021). Our observations show that *P. gombaszoegensis* shares similarities with not one but several different pantherines: both *P. pardus* and *P. leo* for the upper dentition; *P. onca* for the lower dentition; and generally larger pantherines for the cranium as a whole. The morphological evidence presented in

this study therefore advocates for an 'ecological generalist' niche for *P. gombaszoegensis*, which is highly consistent with the large geographical range of the taxon throughout the Pleistocene (cf. Fig. 1A and S1).

Conclusions

Panthera gombaszoegensis is a ubiquitous felid in the Pleistocene of Eurasia. However, many aspects of its morphology are mysterious, owing to the incompleteness of most published remains. Our examination of the near-complete cranium of the *P. gombaszoegensis* ULg-PA-BR-II-81-146 specimen revealed similarities with the extant jaguar *P. onca*, but also highlighted common morphological features with other extant members of Pantherinae. We also found a large number of evidences that support phenotypic differences between *P. onca* and *P. gombaszoegensis,* that comfort the status of *P. gombaszoegensis* as a valid pantherine species, rather than as a subspecies of jaguar. Our morphometric analyses provide a potential explanation for the historic interpretation of *P. gombaszoegensis* as a jaguar, with the lower dentition being extremely similar to that of *P. onca*. Nevertheless, the upper dentition and cranial proportions are far more variable and do not suggest strong affinity to *P. onca* as previously thought. The behaviour of *P. gombaszoegensis* has often been inferred based on its supposed relationship with *P. onca*; our description and analyses show a combination of different pantherine traits, advocating for a more 'generalist' taxa. Finally, our phylogenetic analyses place *P. gombaszoegensis* as the sister taxon to the extant tiger (*P. tigris*), further from the extant jaguar (*P. onca*). This phylogenetic hypothesis simplifies the biogeographic dispersal scenario of this taxon, which is only found in Eurasia, whereas *P. onca* is endemic to the American continent. Under this new scenario, *P. gombaszoegensis* reached Southern Asia approximately in between 1 and 1.8 Myr and did not reach North America. The close affinity between *P. tigris* and *P. gombaszoegensis* thus enables us to propose the presence of a stem tiger in the Pleistocene of Europe, casting doubt on the Asian origin of *P. tigris* and abolishing the misnomer of *P. gombaszoegensis* as a "European jaguar"

Data archiving statement

Data archiving statement. 3D models of the fossil material from the palaeontology collections of the University of Liège are available on MorphoSource (https://www.morphosource.org/projects/000445179) ; Appendix S5 lists all associated DOIs. Associated data (Excel file containing the measurements and ratios, nexus file containing the phylogenetic matrix) and the R script used are provided as Supporting Information, and are available on the University of Liège institutional repository ORBi (https://hdl.handle.net/2268/294237) and MorphoBank

(http://morphobank.org/permalink/?P4265).

Authors' contributions

NC designed the study. NC and MM collected scan data, photographs and drafted the figures. NC took the measurements and ran the morphometric analyses. VF wrote the TNT scripts for the phylogenetic analyses and NC performed the analyses. All authors contributed to writing the manuscript, and gave final approval for publication.

Supporting information

Additional Supporting Information can be found online (https://doi.org/10.1111/spp2.1464):

Appendix S1. Includes TNT script, Figures S1–S10 and Tables S1–S9.

Appendix S2. R script.

Appendix S3. Nexus file containing the phylogenetic matrix.

Appendix S4. README file to explain data.

Appendix S5. List of MorphoSource DOIs associated with this publication.

Data S1. Measurements used in this study.

Acknowledgements

For access to the collections that allowed to compare the *P. gombaszoegensis* material to extant pantherines we thank Prof. Geraldine Véron (MNHN, Paris) and Dr. Emmanuel Gilissen (RMCA, Tevruren). For access to the Otto Zdansky collection from the Uppsala universitet which allowed us to examine the cranium of *P. palaeosinensis* we warmly thank Dr. Benjamin Kear (PMU, Upssala, Sweden). For sharing the 3D model of the *P. spelaea* and '*P.' blythae* crania we thank respectively Dr. Davide Tamagnini (Sapienza University, Rome), Prof. Z. Jack Tseng (UC Berkeley IB/UCMP, Berkeley). We are immensely grateful to Dr. Anne-Claire Fabre for additional pictures of *Panthera uncia* which allowed us to draw figures 4 to 7. For taking great care of fossil remains from La Belle-Roche in their respective institutions we thank Jean-Luc Schütz (Le Grand Curtius Museum, Liège) and Amandine Leusch (Musée du Pays d'Ourthe-Amblève, Comblain).

For their advices during the construction of the project we thank Dr. Manuel J. Salesa (MNCN, Madrid) and Prof. Z. Jack Tseng (UC Berkeley IB/UCMP, Berkeley). NC is supported by a grant of Fonds de la Recherche Scientifique F.R.S.–FNRS (FRIA grant number FC 36251). VF is supported by a grant of Fonds de la Recherche Scientifique F.R.S.–FNRS (MIS F.4511.19). MM is supported by a Fyssen foundation post-doctoral study grant. We also thank the two anonymous reviewers whose comments/suggestions helped improve and clarify this manuscript as well as the editors Dr. Mary Silcox and Dr. Sally Thomas for the time they invested in our manuscript. Finally, we thank our colleague, Dr. Jamie MacLaren, for his diligent proofreading of an earlier version of this manuscript.

References

ANDERSON, M. J. 2001. A new method for non-parametric multivariate analysis of variance. *Austral Ecology*, **26**, 32–46.

ARGANT, A. and ARGANT, J. 2011. The *Panthera gombaszogensis* story: The contribution of the château breccia (Saône-Et-Loire, Burgundy, France). *Quaternaire, Supplement*, 247–269.

BAPST, D. W. 2012. paleotree: an R package for paleontological and phylogenetic analyses of evolution. *Methods in Ecology and Evolution*, **3**, 803–807.

BARNETT, R., MENDOZA, M. L. Z., SOARES, A. E. R., HO, S. Y. W., ZAZULA, G., YAMAGUCHI, N., SHAPIRO, B., KIRILLOVA, I. V., LARSON, G. and GILBERT, M. T. P. 2016. Mitogenomics of the extinct cave lion, *Panthera spelaea* (Goldfuss, 1810), resolve its position within the panthera cats. *Open Quaternary*, **2**, 1–11.

BARONE, R. 1986. *Anatomie comparée des mammifères domestiques, Tome 1, Ostéologie*. Vigot, Paris.

BELL, M. A. and LLOYD, G. T. 2015. strap: an R package for plotting phylogenies against stratigraphy and assessing their stratigraphic congruence. *Palaeontology*, **58**, 379–389.

BEVER, G. S. 2005. Morphometric variation in the cranium, mandible, and dentition of *Canis latrans* and *Canis lepophagus* (Carnivora: Canidae) and its implications for the identification of isolated fossil specimens. *The Southwestern Naturalist*, **50**, 42–56.

BILLET, G. and BARDIN, J. 2019. Serial homology and correlated characters in morphological phylogenetics: Modeling the evolution of dental crests in placentals. *Systematic Biology*, **68**, 267–280.

BONIFAY, M. F. 1971. Carnivores quaternaires du Sud-Est de la France. Mémoires du Muséum national d'Histoire naturelle **21(2)**.

BOULE, M. 1906. Les grands chats des cavernes. *Annales de Paléontologie*, **1**, 69–95.

BOWDICH, E. T. 1821. *An analysis of the natural classifications of Mammalia, for the use of students and travellers*. J. Smith, Paris.

CHRISTIANSEN, P. 2008. Cladistics Phylogeny of the great cats (Felidae : Pantherinae), and the influence of fossil taxa and missing characters. **24**, 977–992.

——— and HARRIS, J. M. 2009. Craniomandibular morphology and phylogenetic affinities of *Panthera atrox*: Implications for the evolution and paleobiology of the lion lineage. *Journal of Vertebrate Paleontology*, **29**, 934–945.

CORDY, J.-M., BASTIN, B., DEMARET-FAIRON, M., EK, C., GEERAERTS,

R., GROESSENS-VAN DYCK, M.-C., OZER, A., PEUCHOT, R., QUINIF, Y., THOREZ, J. and ULRIX-CLOSSET, M. 1993. La grotte de la Belle-Roche (Sprimont, Province de Liège) : un gisement paléontologique et archéologique d'exception au Benelux. *Bulletin de l'Académie royale de Belgique*, **4**, 165–186.

——— and ULRIX-CLOSSET, M. 1991. Synthèse des denrières campagnes de sauvetage du gisement du paléolithique inférieur de La Belle Roche (Sprimont). *Notae Praehistoricae*, **10**, 3–13.

DÁVALOS, L. M., VELAZCO, P. M., WARSI, O. M., SMITS, P. D. and SIMMONS, N. B. 2014. Integrating incomplete fossils by isolating conflicting signal in saturated and non-independent morphological characters. *Systematic Biology*, **63**, 582–600.

DIXON, P. 2003. VEGAN, a package of R functions for community ecology. *Journal of Vegetation Science*, **14**, 927–930.

DRAILY, C. and CORDY, J. 1997. L'industrie lithique de La Belle-Roche à Sprimont (Liège, Belgique) : Paléolithique inférieur. *Notae Praehistoricae*, **17**, 11–20.

DUMBÁ, L. C. C. S., RODRIGUES, F. H. G., MACLAREN, J. A. and COZZUOL, M. A. 2022. Dental occlusal surface and seed dispersal evolution in *Tapirus* (Mammalia: Perissodactyla). *Biological Journal of the Linnean Society*, **136**, 23–40.

EVANS, H. E. and LAHUNTA, A. de. 2013. *Miller's Anatomy of the dog*. Elsevier.

FISCHER, G. 1821. Adversaria zoologica. *Mémoires de la Société impériale des naturalistes de Moscou*, **5**, 357–428.

FISCHER, V., BENSON, R. B. J., ZVERKOV, N. G., SOUL, L. C., ARKHANGELSKY, M. S., LAMBERT, O., STENSHIN, I. M., USPENSKY, G. N. and DRUCKENMILLER, P. S. 2017. Plasticity and convergence in the evolution of short-necked plesiosaurs. *Current Biology*, **27**, 1667-1676.e3.

GASCOYNE, M. and SCHWARCZ, H. P. 1985. Uranium-Series dates for the Lower Paleolithic site of Belle Roche, Belgium. *Current Anthropology*, **26**, 641–642.

GERAADS, D. and PEIGNÉ, S. 2017. Re-Appraisal of '*Felis*' *pamiri* Ozansoy, 1959 (Carnivora, Felidae) from the Upper Miocene of Turkey: the Earliest Pantherin Cat? *Journal of Mammalian Evolution*, **24**, 415–425.

GOLOBOFF, P. A. and CATALANO, S. A. 2016. TNT version 1.5, including a full implementation of phylogenetic morphometrics. *Cladistics*, **32**, 221–238.

———, TORRES, A. and ARIAS, J. S. 2017. Weighted parsimony

outperforms other methods of phylogenetic inference under models appropriate for morphology. .

———, FARRIS, J. S., KÄLLERSJÖ, M., OXELMAN, B., RAMIACUTE;REZ, M. J. and SZUMIK, C. A. 2003. Improvements to resampling measures of group support. *Cladistics*, **19**, 324–332.

GROVES, C. P. 1992. How old are subspecies?: A tiger's eye-view of human evolution. *Archaeology in Oceania*, **27**, 153–160.

HANKÓ, P. E. 2007. A revision of three Pleistocene subspecies of *Panthera*, based on mandible and teeth remains, stored in Hungarian collections. *Fragmenta Palaeontologica Hungarica*, **24**–**25**, 25–43.

HEMMER, H. 1968*a*. Der tiger-*Panthera tigris palaeosinensis* (Zdansky, 1924)-im Jungpleistozan Japans. *Neues Jahrbuch fur Geologie und Palaontologie, Monatshefte*, **1968**, 610–618.

———. 1968*b*. Zur stellung des Tigers (*Panthera tigris*) der Insel Bali. *Zeitschrift für Säugetierkund*, **34**, 216–223.

———. 1971. Zur Charakterisierung und stratigraphischen Bedeutung von *Panthera gombaszoegensis* (Kretzoi, 1938). *Neues Jahrbuch für Geologie und Paläontologie Monatshefte*, **12**, 701–711.

———. 1981. Die Evolution der Pantherkatzen. Modell zur Überprüfung der Brauchbarkeit der Hennigschen Prinzipien der phylogenetischen Systematik für wirbeltier-paläontologische Studien. *Paläontologische Zeitschrift*, **55**, 109–116.

———. 1987. *The phylogeny of the tiger (Panthera tigris)*. Noyes Publication.

——— and KAHLKE, R. 2005. Nachweis des Jaguars (*Panthera onca gombaszoegensis*) aus dem späten Unter-oder frühen Mittelpleistozän der Niederlande. *Deinsea*, 47–57.

———, KAHLKE, R.-D. and VEKUA, A. K. 2001. The Jaguar - *Panthera onca gombaszoegensis* (Kretzoi, 1938) (Carnivora: Felidae) in the late lower pleistocene of Akhalkalaki (south Georgia; Transcaucasia) and its evolutionary and ecological significance. *Geobios*, **34**, 475–486.

———, ——— and ———. 2010. *Panthera onca* georgica ssp. nov. from the Early Pleistocene of Dmanisi (Republic of Georgia) and the phylogeography of jaguars (Mammalia, Carnivora, Felidae). *Neues Jahrbuch fur Geologie und Palaontologie - Abhandlungen*, **257**, 115–127.

HERRINGTON, S. J. 1987. Subspecies and the conservation of *Panthera tigris*: preserving genetic heterogeneity. *In* TILSON, R. and SEAL, U. (eds.) *Tigers of the World: The Biology, Biopolitics, Management and Conservation of*

an Endangered Species, Noyes Publication, Park Ridge, 51–63 pp.

JANEČKA, J. E., JACKSON, R., YUQUANG, Z., DIQIANG, L., MUNKHTSOG, B., BUCKLEY-BEASON, V. and MURPHY, W. J. 2008. Population monitoring of snow leopards using noninvasive collection of scat samples: a pilot study. *Animal Conservation*, **11**, 401–411.

JENNINGS, H. S. and REIGHARD, J. 2019. *Anatomy of the cat*. Good Press.

JERNVALL, J. 2000. Linking development with generation of novelty in mammalian teeth. *PNAS*, **97**, 2641–2645.

——— and JUNG, H.-S. 2000. Genotype, phenotype, and developmental biology of molar tooth characters. *Yearbook of physical antropology*, **43**, 171–190.

JIANGZUO, Q. and LIU, J. 2020. First record of the Eurasian jaguar in southern Asia and a review of dental differences between pantherine cats. *Journal of Quaternary Science*, **35**, 817–830.

———, WANG, Y., GE, J., LIU, S., SONG, Y., JIN, C., JIANG, H. and LIU, J. 2022. Discovery of jaguar from northeastern China middle Pleistocene reveals an intercontinental dispersal event. *Historical Biology*, 1–10.

JOHNSON, W. E., EIZIRIK, E., PECON-SLATTERY, J., MURPHY, W. J., ANTUNES, A., TEELING, E. and O'BRIEN, S. J. 2006. The late miocene radiation of modern felidae: A genetic assesstment. *Science*, **311**, 73–77.

KING, L. M. and WALLACE, S. C. 2014. Phylogenetics of *Panthera*, including *Panthera atrox*, based on craniodental characters. *Historical Biology*, **26**, 827–833.

KITCHENER, A. C. and YAMAGUCHI, N. 2010. What Is a Tiger? Biogeography, Morphology, and Taxonomy. December. *In* TILSON, R. and NYHUS, P. (eds.) *Tigers of the World*, Elsevier, 53–84 pp.

KLINGENBERG, C. P. 1996. Multivariate Allometry. *In* MARCUS, L., CORTI, L., LOY, A., NAYLOR, G. and SLICE, D. (eds.) *Advances in Morphometrics*, Springer, Boston, 23–49 pp.

KRETZOI, M. 1938*a*. Die Raubtiere von Gombaszög nebst einer Übersicht der Gesamtfauna. *Annales Musei Nationalis Hungarici, Pars Mineralogica, Geologica, Palaeontologica*, **31**, 88–157.

———. 1938*b*. Die Raubtiere von Gombaszog nebst einer Übersicht der Gesamtfauna. *Geologic Paleontology*, **31**, 88–157.

KRETZOI, M. 1945. Bemerkungen über das Raubtiersystem. *Annales historico-naturales Musei nationalis hungarici*, **38**, 59–83.

KURTÉN, B. 1973. Pleistocene jaguars in North America. *Commentations Biologica*, **62**, 1–23.

LANGLOIS, A. 2002. Présence de *Panthera gombaszoegensis* Kretzoï, 1938 à la grotte xiv (Cénac-et-Saint-Julien, Dordogne). *Paléo*, 213–220.

LEGENDRE, P. and LEGENDRE, L. 1998. *Numerical ecology*. 2nd edition. Developments in Environmental Modelling, 20. Elsevier.

LEROY, A., MONTUIRE, S. and MARCHAND, D. 2004. Analysis of teeth outlines: a morphometric tool for distinguishing three species of Crocidurinae (Soricidae, Insectivora, Mammalia) in France. *Journal of Natural History*, **38**, 259–267.

LINNAEUS, C. 1758. *Systema naturae*. Vol. 1. Laurentii Salvii, Stockholm.

MADDISON, W. P. and MADDISON, D. R. 2019. Mesquite: a modular system for evolutionary analysis, ver. 2.72. *Ci.nii.ac.jp*. http://www.mesquiteproject.org

MARCISZAK, A. 2014. Presence of *Panthera gombaszoegensis* (Kretzoi, 1938) in the late middle pleistocene of biśnik cave, Poland, with an overview of Eurasian jaguar size variability. *Quaternary International*, **326**–**327**, 105–113.

——— and LIPECKI, G. 2021. *Panthera gombaszoegensis* (Kretzoi, 1938) from Poland in the scope of the species evolution. .

MARTIN, L. D. and GILBERT, B. 1978. An american lion, *Panthera atrox*, natural trap Cave, north central Wyoming. *Rocky Mountain Geology*, **16**, 95–101.

MAZÁK, J. H. 1981. *Panthera tigris*. *Mammalian species*, 1–8.

MAZÁK, J. H. 2010. What is *Panthera palaeosinensis*? *Mammal Review*, **40**, 90–102.

MAZÁK, J. H. and GROVES, C. P. 2006. A taxonomic revision of the tigers (*Panthera tigris*) of Southeast Asia. *Mammalian Biology*, **71**, 268–287.

MAZÁK, J. H., CHRISTIANSEN, P. and KITCHENER, A. C. 2011. Oldest known pantherine skull and evolution of the tiger. *PloS one*, **6**, e25483.

MELCHIONNA, M., PROFICO, A., CASTIGLIONE, S., SERIO, C., MONDANARO, A., MODAFFERI, M., TAMAGNINI, D., MAIORANO, L., RAIA, P., WITMER, L. M., WROE, S. and SANSALONE, G. 2021. A method for mapping morphological convergence on three-dimensional digital models: the case of the mammalian sabre-tooth. *Palaeontology*, **64**, 573–584.

MERRIAM, J. C. 1909. The skull and dentition of an extinct cat closely allied to *Felis atrox* Leidy. *Bulletin of the Department of Geology*, **5**, 291–304.

MOL, D., LOGCHEM, W. Van and VOS, J. De. 2011. New record of the

European jaguar, *Panthera onca gombaszoegensis* (Kretzoi, 1938), from the Plio-Pleistocene of Langenboom (The Netherlands). *Cainozoic Research*, **8**, 35–40.

NAYLOR, G. J. P. and ADAMS, D. C. 2001. Are the fossil data really at odds with the molecular Data? Morphological evidence for Cetartiodactyla phylogeny reexamined. *Systematic biology*, **50**, 444–453.

O'REGAN, H. J. 2002. A phylogenetic and palaeoecological review of the Pleistocene felid *Panthera gombaszoegensis.* PhD thesis, Liverpool John Moores University, 349 pp. https://doi.org/10.24377/LJMU.t.00004925

O'REGAN, H. J. and TURNER, A. 2004. Biostratigraphic and palaeoecological implications of new fossil felid material from the Plio-Pleistocene site of Tegelen, The Netherlands. *Palaeontology*, **47**, 1181–1193.

OKEN, L. 1816. *Okens Lehrbuch der Naturgeschichte (Volume 3, part 1)*. 3 [1]. Reclam C.H.

PARADIS, E. and SCHLIEP, K. 2019. Ape 5.0: An environment for modern phylogenetics and evolutionary analyses in R. *Bioinformatics*, **35**, 526–528.

REPENNING, C. A., WEASMA, T. R. and SCOTT, G. R. 1995. The Early Pleistocene Latest Blancan-Earliest Irvingtonian) Froman Ferry Fauna and History of the Glenns Ferry Formation, Southwestern Idaho. *U.S. GEOLOGICAL SURVEY BULLETIN*, **2105**.

REYNOLDS, B. 2013. Determiners, feline marsupials, and the category-function distinction: A critique of ELT grammars. *TESL Canada Journal*, **30**, 1.

ROEBROEKS, W. and STAPERT, D. 1986. On the 'Lower Paleolithic' Site La Belle Roche : An alternative interpretation. *Current Anthropology*, **27**, 369–371.

SANSOM, R. S., ALBION WILLS, M. and WILLIAMS, T. 2017. Dental data perform relatively poorly in reconstructing mammal phylogenies: Morphological partitions evaluated with molecular benchmarks. *Systematic biology*, **66**, 813–822.

SCHALLER, O., CONSTANTINESCU, G. M., HABEL, R. E., SACK, W. O., SIMOENS, P. and DE VOS, N. R. 2007. *Illustrated veterinary anatomical nomenclature*. *In* SCHALLER, O. (ed.) Enke Verlag, Stuttgart.

SEYMOUR, K. L. 1989. Panthera onca. *Mammalian Species*, 1–9.

SLATER, G. J. and VAN VALKENBURGH, B. 2009. Allometry and performance: The evolution of skull form and function in felids. *Journal of Evolutionary Biology*, **22**, 2278–2287.

SOTNIKOVA, M. and NIKOLSKIY, P. 2006. Systematic position of the cave lion *Panthera spelaea* (Goldfuss) based on cranial and dental characters. *Quaternary International*, **142**–**143**, 218–228.

SOTNIKOVA, M. S. 1990. Pleistocene mammals from Lakhuti, Southern Tajikistan, USSR. *Quatärpaläontologie*, 237–244.

STIMPSON, C. M., BREEZE, P. S., CLARK-BALZAN, L., GROUCUTT, H. S., JENNINGS, R., PARTON, A., SCERRI, E., WHITE, T. S. and PETRAGLIA, M. D. 2015. Stratified Pleistocene vertebrates with a new record of a jaguar-sized pantherine (*Panthera* cf. *gombaszogensis*) from northern Saudi Arabia. *Quaternary International*, **382**, 168–180.

STOCK, D. W. 2001. The genetic basis of modularity in the development and evolution of the vertebrate dentition. *Philosophical Transactions of the Royal Society* , **356**, 1633–1653.

TAMAGNINI, D., MELORO, C. and CARDINI, A. 2017. Anyone with a Long-Face? Craniofacial Evolutionary Allometry (CREA) in a Family of Short-Faced Mammals, the Felidae. *Evolutionary Biology 2017 44:4*, **44**, 476–495.

TSENG, Z. J., WANG, X., SLATER, G. J., TAKEUCHI, G. T., LI, Q., LIU, J. and XIE, G. 2013. Himalayan fossils of the oldest known pantherine establish ancient origin of big cats. *Proceedings of the Royal Society B: Biological Sciences*, **281**, 1–7.

TURNER, A. and ANTÓN, M. 1997. *The big cats and their fossil relatives: an illustrated guide to their evolution and natural history*. Columbia University Press.

UNGAR, P. S. 2010. *Mammal Teeth: Origin, Evolution, and Diversity*. John Hopkins University Press.

YIQING, M. and YAN, X. 2010. On the origin of tigers in China and process of endanger. *Chinese journal of wildlife*, **31**, 262–269.

ICVGAN 2017. *Nomina Anatomica Veterinaria*. 6th edition. International Committee on Veterinary Gross Anatomical Nomenclature. http://www.wava-amav.org